Prof. A. R. Biswas (Bombay)

Copy to Library

COMPUTERISED

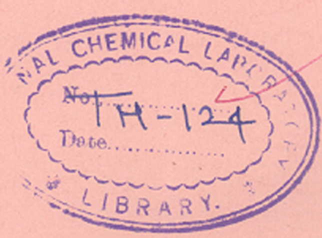

STRUCTURAL, ELECTRICAL AND OPTICAL PROPERTIES OF SOME SEMICONDUCTING CHALCOGENIDES

COMPUTERISED

A thesis submitted to
THE UNIVERSITY OF POONA
for the degree of
DOCTOR OF PHILOSOPHY
(IN CHEMISTRY)

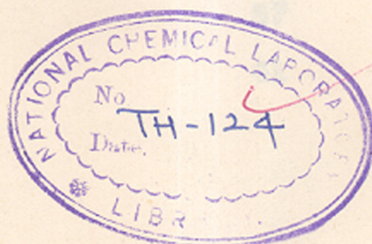

537.311.33 (043)
KHA

By
R.R.KHANDEKAR
M.Sc.

National Chemical Laboratory, Poona - 8.

1975

C O N T E N T S

	Page
GENERAL INTRODUCTION	1
CHAPTER- 1	
ARSENIC TELLURIDE	
Historical background	4
Experimental techniques	11
Results	27
Discussion	37
References	41
CHAPTER - 2	
ARSENIC SELENIDE	
Historical background	43
Crystalline Arsenic tetraselenide	
Experimental techniques	51
Results	53
Amorphous Arsenic tetraselenide	
Introduction	60
Experimental techniques and results	65
Discussion	82
References	87

Page

CHAPTER- 3

ANTIMONY TELLURIDE

Historical background	90
Experimental techniques	96
Results	100
Discussion	1O6
References	111

CHAPTER - 4

ANTIMONY SELENIDE

Historical background	112
Experimental techniques	122
Results	123
discussion	127
References	129

CHAPTER -5

CADMIUM TELLURIDE

Historical background	131
Experimental techniques	135
Results	136
Discussion	140
References	142

Page

CHAPTER - 6

CADMIUM SELENIDE

Historical background	144
Experimental techniques	147
Results	148
Discussion	152
References	156

CHAPTER - 7

SUMMARY AND CONCLUSIONS	158

________ o __________

GENERAL INTRODUCTION

Chalcogenide semiconductors have recently been the focus of considerable attention because of their switching and memory effects. These disordered materials find applications in optics, electronics, electrophotography. The chalcogenide glasses are of particular interest because of their increasing use in electrostatic imaging, television engineering and switching and memory devices.

Amorphous selenium films are currently used in xerography[1,2] because of their relatively high stability, high photoconductivity, and the low equilibrium conductivity. Amorphous antimony sulfide and also arsenic selenide[4] are used in wellknown vidicon tubes. Some of the amorphous films, by virtue of their instability[5] caused by crystallization or vitrification, are put to use in fabricating memory devices. The vitrifiable materials (e.g. Te-As-Ge) are used in resettable memory devices. Especially the laser beam induced structural changes in amorphous semiconducting films are used to store and convey information[6-8]. Another device based on such instability is a threshold switch[9-16]. It is different from memory switch in that it does not lock in the 'ON' state but switches back below a certain holding current into 'OFF' state. The above mentioned switching devices are used in electronic circuitry[17-19], in display by electroluminescent panels[20], in computer memories[20], for linear amplification

in some special circuits[18], also as a piezoelectric sensor[21].

Certain semiconductors can be made amorphous under drastic quenching conditions, such as vapour deposition onto a cold substrate. In case of arsenic and antimony chalcogenides a serious problem arises of controlling stoichiometry or of maintaining a constant predetermined composition of deposited materials.

One aim of the present work has been to develop a chemical method for the preparation of thin films of arsenic, antimony and cadmium chalcogenides. The same method can be made suitable for preparing mixed solid solutions also. (e.g. $As_2Te_3.As_2Se_3$; $Sb_2Se_3.Sb_2Te_3$ etc.). However the scope of this thesis is restricted to only arsenic, antimony and cadmium chalcogenides (simple binary selenides and tellurides) prepared by this chemical method and vitreous arsenic tetraselenide prepared by melt quenching. Throughout the work described in this contribution, the intent has been to compare the properties of the vitreous, amorphous and crystalline thin films obtained by this chemical method with those of the films obtained by the other conventional methods.

This thesis comprises of seven different chapters; the first six chapters deal with different compounds; arsenic telluride, arsenic selenide, antimony telluride, antimony selenide, cadmium telluride and cadmium selenide.

Each chapter is further subdivided in different sections, covering the historical survey of the individual compound, the experimental techniques used, the results obtained and conclusions and discussions.

The overall summary and conclusions are given at the end in the seventh chapter.

CHAPTER - 1.

ARSENIC TELLURIDE

1.1 Historical Background

The unit cell of As_2Te_3 is monoclinic and the space group is C^3_{2h} - C2/m [22]. The lattice parameters are

$a = 14.339 \pm 0.001$ Å, $b = 4.006 \pm 0.005$ Å,
$c = 9.873 \pm 0.005$ Å, $\beta = 95.0^\circ$.

There are four molecules per unit cell. The atoms occupy five sets of special positions as follows:

$4(i) : (x, 0, z)\ (\bar{x}, 0, \bar{z}) + (0, 0, 0;\ 1/2, 1/2, 0)$

Atomic positional parameters :

	x	y	z
As_I	0.115	0.5	0.445
As_{II}	0.205	0.0	0.145
Te_I	0.032	0.0	0.282
Te_{II}	0.280	0.5	0.337
Te_{III}	0.375	0.0	0.034

The structure, which consists of zigzag chains in which the arsenic atoms are octahedrally and trigonally bonded to telluriums, appears closely related to the structure of β-Ga_2O_3 [23].

T.C.Harman et al.[24] published a paper on the preparation of tellurides from purified elements by several techniques and presented the data on electrical and thermal properties of n-type ('Te' doped) and p-type As_2Te_3 ('As' doped) as a function of temperature and impurity concentration. Pressure contacts to As_2Te_3 were found to give spurious results. Tin soldered contacts were used to give consistent reproducible results. Electrical resistivity was measured for polycrystalline, cylindrically shaped specimens from 80 to 250°K. Intrinsic resistivity region was not attained because of the high impurity concentration of the specimens. The variation of carrier mobility with temperature was approximately proportional to $T^{-5/2}$ for As_2Te_3. This led to the conclusion that the compounds were necessarily heavily doped.

B.T.Kolomiets[25] found that the conductivity of such chalcogenides glasses increased with the increase in the proportion of the heavy component. Many glasses were found to pass easily to a crystalline state by annealing in the softening range. This transition caused very large changes in conductivity. Such high differences in conductivity between the glassy and crystalline state of the same material were attributed to a change in the short range order or to the changes in the impurity states on transition.

K.Weiser and M.H.Brodsky[26] studied the electrical conductivity, optical absorption and photoconductivity of amorphous As_2Te_3 films prepared by condensing the vapour on a cooled substrate. Over the temperature range 200 to 400^oK the conductivity was of the form $\sigma = \sigma_o \exp(-Ea/kT)$, with $\sigma_o = 600\ \Omega^{-1}cm^{-1}$ and Ea = 0.4 ev. The results were interpreted in terms of a "conductivity gap" of 0.8 ev. The average mobility was found to lie between 0.3 and 5 cm^2/v.sec., which led to the fact that the "mobility edges*" which are responsible for the conductivity gap were on the border-line between localized and delocalized states. The optical absorption data supported the fact that for energies well above the conductivity gap the density of valence and conduction band states had a parabolic dependence on energy. The experimentally found optical gap of 0.95 - 0.98 ev was the energy difference between edges of parabolic states. Photoconductivity measurements gave the lower limit of mobility of carriers to be 0.3 cm^2/v.sec.

---

* Footnote : Mobility edges are the regions of energy where the mobility of carriers increases quite abruptly from a negligible value to a value which no longer depends strongly on energy.

N.Croitoru et al.[27] studied the electrical conductivity of amorphous thin films of As_2Te_3 and at low and high electrical fields in temperature range from 77 to 350°K. The value of Ea = 0.25 ev at 400 volts while the value at 10 volts was 0.46 ev. There was a space charge limited current with a trap level located at 0.28 ev.

H.K.Rockstad[28] studied the frequency dependence of the ac conductivity of As_2Te_3 at room temperature. The conductivity could be considered to consist of 2 components, a frequency independent component σ_o and a frequency (w) dependent component σ_1. He found σ_1 varied as w^s with 's' usually lying in the range 0.8 to 0.9. The component σ_1 is attributed to a hopping mechanism, and σ_o is attributed to intrinsic band conduction. Optical data for the fundamental absorption edge were also included.

A.Hrubý and L.Štourač[29] studied DTA and electrical conductivity of glassy semiconducting As_2Te_3. Electrical conductivity was measured in the range 150 to 300°K and it was found that the temperature dependence of conductivity was exponential from 200 to 300°K, expressed by the relation $\sigma = \sigma_o \exp(-Eg/2kT)$ where Eg = 0.95 ev. These measurements were done with the electric fields upto 100 v/cm on samples with variable geometry in order to eliminate the contact resistance.

H.K.Rockstad[30] studied the temperature dependence of ac and dc conductivity. The quantity $(\sigma_1 \equiv \sigma - \sigma_o)$ was plotted as a function of temperature at 10^5 Hz; where σ_1 was ac component and σ_o was dc component of the conductivity. Below 200°K σ_1 was proportional to $T w^s$ and above 200°K it rose more rapidly with T. At any given temperature σ_1 was proportional to w^s where $s \simeq 1$. The quantity σ_1 was attributed to hopping in localized states and in tail states near mobility edges. The plot log σ_o - 1/T was linear for σ_o between 10^{-8} and 10^{-3} ohm^{-1} cm^{-1} with an activation energy 0.39 ev.

J.M.Marshall et al.[31] reported the transport and photoconductivity properties of non-crystalline As_2Te_3 and correlated the data with the band structure of the material. The log σ - 1/T plot showed several regions with differing activation energies. The low field value of 0.42 ev decreased to about 0.30 ev at high fields, with a further reduction to about 0.22 ev at low temperatures. Temperature dependence of the photocurrent gave rise to activation energies of 0.16 ev and 0.11 ev in the low temperature region. Bimolecular recombination analysis suggested that traps were at depths of 0.32 ev and 0.22 ev which tallied with the high field data. (Room temperature value of drift mobility of As_2Te_3 $10^{-2} cm^2/v$ x sec. and Ea = .35 - .40 ev).

L.Štourač et al.[32] studied the optical absorption and photoconductivity of As_2Te_3 glass as a function of photon energy and temperature. DC electrical conductivity was measured by a two probe arrangement at fields lower than 10 v/cm and was found to be exponentially dependent on 1/T i.e. $\sigma = \sigma_o \exp(-Eg/2kT)$. Here Eg = 0.90 ev at 300°K and $\sigma_o = 10^3\ \Omega^{-1}cm^{-1}$. The value of Eg matches with the bandgap of As_2Te_3 which indicates that it is the activation energy of intrinsic conductivity. Below 200°K there was a deviation from the exponential dependence which was explained as due to the intrinsic conductivity being gradually replaced by the hopping conductivity.

A.Abrahám et al.[33] studied the optical absorption, photoconductivity, electrical conductivity and DTA of glassy As_2Te_3. DC conductivity results are comparable to those reported above[32].

D.Brasen[34] studied low field (10 v/cm) conductivity of glassy films of As_2Te_3 obtained by splat-cooling of crystalline As_2Te_3. He obtained Ea = 0.3 ev for non-annealed samples. After annealing the films above 85°C, he found an increase in the activation energy. The films annealed at 112°C gave Ea = 0.475 ev.

K.Weiser, A.J.Grant and T.D.Moustakas[35] published an extensive work on the transport properties of amorphous arsenic telluride. They developed a model for the conduction in localized band-tail and in extended states which implied that the amorphous solid conduction was dominated by carriers in localized states. They studied the low and high field conductivity, thermopower, photoconductivity and Hall effect. Activation energy calculated from the conductivity vs temperature curve was found to be 0.45 ev.

1.2 Experimental techniques

Preparation of thin films of arsenic telluride

Thin films of arsenic telluride (As_2Te_3) were prepared by the action of hydrogen telluride gas on an aqueous solution of arsenic trichloride. The method of preparation is described below.

An aqueous solution of arsenic trichloride was prepared by the method described by J.Devy[36]. Arsenic trioxide was heated in a mixture of concentrated hydrochloric acid and concentrated sulphuric acid. The prepared solution was then diluted to desired concentration. The compound, Al_2Te_3, required for the preparation of hydrogen telluride[37](H_2Te), was prepared by melting the stoichiometric mixture of the elements in evacuated silica capsules.

A vacuum desiccator with two openings, each having a stopcock, was used as the reaction vessel (Fig.1). A shallow dish containing solution of $AsCl_3$ was kept in the desiccator. A glass disc with a rod fixed at the edge, was kept in the solution with the disc dipping completely under the solution. A dry tiny bowl, previously heated under ir lamp was placed near the shallow dish exactly under the funnel tip. Then a small amount of Al_2Te_3, which was freshly prepared and preserved under dry conditions in a desiccator, was transferred

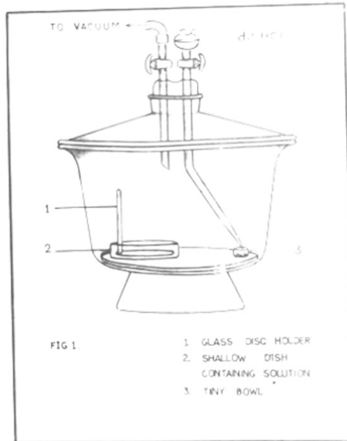

FIG 1.

1. GLASS DISC HOLDER
2. SHALLOW DISH CONTAINING SOLUTION
3. TINY BOWL

to the bowl. The other opening was then connected to the water suction pump. This pre-suction was required to allow the generated gas to diffuse uniformly over the surface of the solution in the dish. After about 15 minutes the suction was cut off and a few drops of dilute HCl were added into the funnel. The stopcock under the funnel was then slowly opened so that dilute HCl could slip down very slowly into the bowl containing Al_2Te_3. The flow of dilute HCl was stopped leaving behind some HCl in the funnel. By this care no air was allowed to enter the vessel through the funnel. The generated gas H_2Te diffused over the entire surface of the solution inside the shallow dish and gave a thin uniform film of arsenic telluride. After a certain time interval the reaction vessel was again connected to the water suction pump to remove most of the unreacted H_2Te gas. After about 30 minutes air was allowed to leak slowly in the system through funnel and flush out the residual H_2Te. The film so formed was then lifted on the glass disc and allowed to refloat on fresh distilled water to wash out the possible water soluble impurities. This washing process was repeated thrice. This film of arsenic telluride was then taken on different substrates as required for different measurements, dried and preserved in a desiccator.

It was found experimentally that the concentration range 0.01 - 0.02M of $AsCl_3$ and a pH range of 2-4 gave good results.

While handling the gas, due care was taken against its toxic behaviour[38]. The gas decomposes in the presence of moisture and rubber, therefore ground glass joints were used wherever needed. The whole experimental set-up was enclosed inside a good hood fixed with a powerful exhaust fan.

Electron diffraction

In order to get an idea about the structure of the film of arsenic telluride, electron diffraction technique was employed. A piece of fine nickel wire gauze was heated to red heat in a flame and cooled. A drop of collodion solution (2%) in amylacetate was added to fresh distilled water in a shallow dish. After some time a thin and transparent film was formed on the surface of water. The film was lifted on the cleaned nickel wire guaze and dried. The washed film of arsenic telluride was taken on this piece of guaze holding the collodion film. It was then dried and a transmission electron diffraction pattern was taken. The arsenic telluride film was also taken on a clean glass substrate and electron diffraction pattern by reflection was taken.

Thickness measurements

The multiple beam interferometery method[39] was employed to measure the thickness of films. The light rays

which have undergone multiple reflections between a substrate and reference flat, interfere and form fringes. These interference fringes, which are sharp because of multiple reflections, are used to determine the film thickness. The fringes produced by multiple beam interferometery are depicted in Fig.2a.

A sharp step was produced between the substrate and the surface of arsenic telluride film. A highly reflecting opaque film of aluminium was then evaporated on it. This deposit accurately contours the step. A partially transparent film of aluminium was deposited on another glass slide. This was the reference plate, placed on the top of the step. This reference plate made small angle to the substrate surface. It was then illuminated with collimated monochromatic light obtained from sodium source (5893 Å). Fringes of equal thickness were then produced where the beams interferred constructively (Fig.2b).

The fringe spacing D, and fringe displacement across the step d, (Fig.2c) were measured with the help of a travelling microscope. Thickness t, of the film of

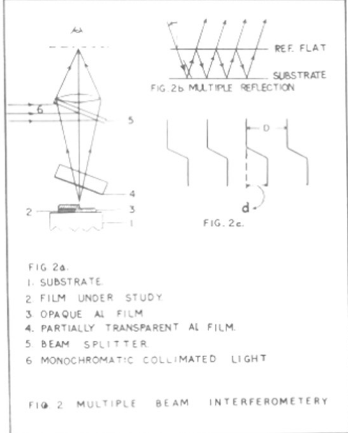

FIG. 2 MULTIPLE BEAM INTERFEROMETERY

TH-124

arsenic telluride was calculated using the formula

$$t = \frac{d}{D} \times \frac{\lambda}{2}$$

where t = thickness of the film

d = fringe displacement

D = fringe spacing

λ = 5893 Å (sodium lamp yellow lines)

I-V characteristics

i) Sample preparation

First the bottom gold electrode was deposited on a glass substrate by vacuum evaporation. The film of arsenic telluride was taken on this electrode with proper maskings. The film was then allowed to dry at about 95°C for half an hour and then preserved in a desicator. These dried films over gold electrodes were masked properly and the top aluminium electrode was deposited by vacuum evaporation. This gave a sandwich structure as follows :

Au - As_2Te_3 - Al (Fig.3a)

ii) Dynamic characteristic

The sandwich, in series with a variable resistance 'R' was connected to a function generator 'F' (Fig.3b).

537.311.33(043)
KHA

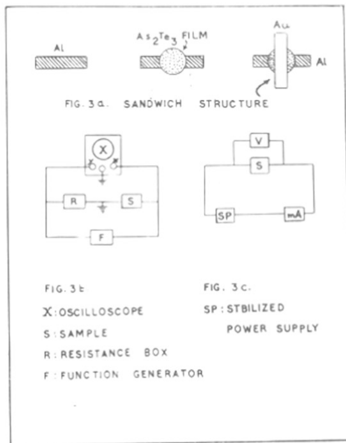

FIG. 3a. SANDWICH STRUCTURE

FIG. 3b

X: OSCILLOSCOPE

S: SAMPLE

R: RESISTANCE BOX

F: FUNCTION GENERATOR

FIG. 3c.

SP: STBILIZED POWER SUPPLY

The voltage drop across the sandwich 'S' was fed to the x-amplifier while the voltage across the resistance was fed to the y-amplifier of the oscilloscope 'X' (Tektronix 515 A). Triângular pulse was used for the measurements. The x- and y- gain of the amplifier were adjusted so as to limit the trace of the beam within the view of the oscilloscope. The oscilloscope was calibrated with the internal calibration signal. As the voltage drop across 'R' was equal to RI, with usual notations, the beam directly traced the I-V characteristic of the sandwich under study.

iii) Steady state characteristic

DC I-V characteristic was also studied using the circuit described in the Fig.3c. The voltage was applied to the sample 'S' from a stabilized power supply 'SP'. By varying the applied voltage the current was recorded from milliameter. A graph of current (I) versus voltage (V) was plotted.

DC electrical conductivity

A two probe arrangement was used to study the electrical conductivity. Gold or aluminium was evaporated

on the thin film with proper masking to give a spacing of one millimeter between the two end electrodes. These coplanar electrodes were given pressure contacts with the help of phosphor bronze strips. The sample holder (Fig.4a) made out of a brass block was provided with a microheater. The sample holder was connected to the bottom of a double-wall pyrex dewar flask with the help of a 'glass-to-metal' seal (Fig.4b). (This multipurpose conductivity cell can be used for conductivity and ir absorption measurements from liquid nitrogen temperature to 400°C. At the bottom of the cell a provision was made to fix two sodium chloride windows on either side).

Through one of the openings in the Dewar, six insulated copper wires (two for microheater and four for conductivity) and two thermocouple wires (copper and constantan) were taken out and then this opening was epoxy-sealed and made leakproof for vacuum of the order of 10^{-4}Torr. At the bottom of this conductivity cell, a B-19 joint was fused which was connected to the vacuum system when needed.

The heater was connected to a stabilized DC power supply. The copper-constantan junction was placed on the film, the thermoemf of which gave the temperature of the sample under study. A stabilized power supply was used to apply a fixed voltage whereas the current flowing through

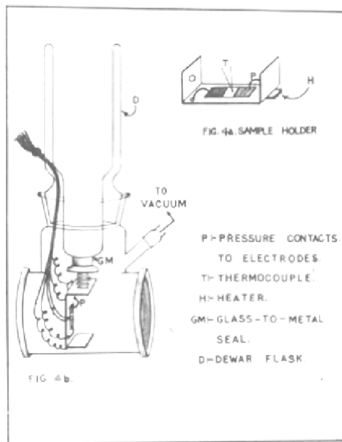
T
P
H
D
FIG. 4a. SAMPLE HOLDER
TO
VACUUM
GM
P
P – PRESSURE CONTACTS
TO ELECTRODES.
T – THERMOCOUPLE.
H – HEATER.
GM – GLASS-TO-METAL
SEAL.
D – DEWAR FLASK
FIG. 4b.

the sample was measured using an electrometer.

The distance between electrodes ('L') and area of cross section ('A') were measured accurately. With the knowledge of 'L', 'A' and 'R' (resistance) the resistivity 'ρ' was calculated by the wellknown relation[40]:

$$\rho = R \times A/L$$

or $$\sigma = L/R \times A$$

where σ = conductivity ($\Omega^{-1}cm^{-1}$).

The graph of log σ vs 1/T was plotted. The slope of this graph gave the value of thermal activation energy, Ea.

By extrapolating the graph to 1/T = 0; the pre-exponential factor σ_o was calculated which appears in the conductivity expression given below.

$$\sigma = \sigma_o \exp(-Ea/kT)$$

where σ = conductivity ($\Omega^{-1}cm^{-1}$)

σ_o = pre-exponential factor ($\Omega^{-1}cm^{-1}$)

Ea = Thermal activation energy

k = Boltzmann's constant

T = Absolute temperature

Optical absorption

The fundamental absorption refers to the excitation of an electron from the valence band to conduction band and it manifests itself by a rapid rise in absorption which can be used to determine the energy gap of the semiconductor.

The absorption coefficient, $\alpha(h\nu)$, for a given photon energy is proportional to the probability for the transition from the initial state to the final state and also to the density of available (empty) final state. The selection rule for the allowed transition is $\Delta k = 0$; i.e. a transition indicated by a vertical line on a plot of E vs k (Direct transition). Phonon assisted indirect transitions ($\Delta k \neq 0$) are also possible but they are in general weaker than the direct ($\Delta k = 0$) transitions.

If exciton formation or electron-hole interaction is neglected, the forms of the absorption coefficient, α, as a function of photon energy $h\nu$ depend on the type of energy bands containing the initial and final state. For simple parabolic bands they are :

For direct transitions :-

$$\alpha h \nu n_o \sim (h\nu - Eg\ opt)^n$$

where $n = \frac{1}{2}$ or 3/2 depending on whether the transition is allowed or forbidden in the quantum- mechanical sense. Eg opt is the optical gap and n_o is the refractive index.

For indirect transitions :

$$\alpha n_o \cdot h\nu \sim \frac{(h\nu - Eg\ opt + Eph)^n}{\exp(Eph/kT) - 1} + \frac{(h\nu - Eg\ opt - Eph)^n}{1 - \exp(-Eph/kT)}$$

Here Eph is the energy of phonon and $n = 2$ for allowed transitions whereas for forbidden transitions $n = 3$. The two terms in the above expression represent contributions from transitions involving phonon absorption and emission respectively. They have different coefficients of proportionality and temperature dependences.

Absorption coefficient for direct transitions[41] usually lies in the range 10^4 to 10^5 cm^{-1} whereas for indirect transitions the range is 10 to 10^3 cm^{-1}. In order to evaluate the band gap for direct allowed transitions α^2 or $(\alpha h\nu)^2$ or $(\alpha h\nu)^{2/3}$ is plotted against photon energy to give a straight line. The intercept of this plot on energy axis gives the band gap (Eg opt).

In case of indirect transitions[41] $\alpha^{\frac{1}{2}}$ or $(\alpha h\nu)^{\frac{1}{2}}$ is plotted against photon energy to give a straight line. Actually two straight lines and hence two intercepts are usually obtained for indirect transitions. One intercept corresponds to (Eg opt + Eph) and the other corresponds to (Eg opt - Eph).

The absorption curve over a wide spectral range exhibits three distinct features[42]. The high energy side portion of the curve corresponds to the interband transition which can be characterized by a rapid rise in absorption coefficient over several decades within a narrow range of photon energy (a few ev) near the forbidden gap. Here the relation $\alpha h\nu \sim (h\nu - E_g\ opt)^n$ holds good.

In several materials like alkali halides, CdS, trigonal Se a different type of absorption edge is observed. There is a gradual increase in the absorption extending over a wide range of photon energy (several ev), (the onset of interband absorption). It is named as Urbach edge or tail which obeys the following relation :

$$\alpha = \alpha_0 \exp \left\{ \gamma' (h\nu - E_g\ opt)/kT \right\}$$

where γ' is constant and T is absolute temperature ($\sim 100^\circ K$). The possible explanation given for this type of behaviour is as due to band edge exciton absorption modified by internal fields. The order of the fields is estimated to be 5×10^5 v/cm. This exponential absorption region is very much alike, bearing same slope, for almost all amorphous and many crystalline semiconductors. Therefore it is not attributed to absorption from and to tail state. On still lower energy side very weak absorption is observed. This region is sensitive to the structure and composition of the material under study. Its

behaviour is also exponential with photon energy and is apparently associated with absorption involving gap states.

The film of arsenic telluride was taken on a quartz substrate. Using another blank quartz plate of the same thickness as the reference, the optical spectrum of the film was scanned on a ratio recording Beckmann spectrophotometer. The spectrum was scanned in the spectral range 500 to 1300 mμ. Absorption coefficient, α, at different photon energies ($h\nu$) was calculated using the formula[43],

$$\alpha = \frac{2.303 \log_{10} I_0/I_x}{\text{thickness } (x)} = \frac{2.303 \text{ x optical density}}{\text{thickness of the film in cms.}}$$

In order to determine the optical activation energy and the type of optical transition various graphs were plotted such as $\log\alpha$ vs $h\nu$, α^2 vs $h\nu$, $\sqrt{\alpha}$ vs $h\nu$, $\sqrt{\alpha h\nu}$ vs $h\nu$, $(\alpha h\nu)^2$ vs $h\nu$, $(\alpha h\nu)^{2/3}$ vs $h\nu$ etc.

1.3 Results

Electron diffraction

Fig.5 displays the electron diffraction patterns, obtained by transmission and by reflection, for arsenic telluride film.

The 'd' values and the relative intensities for the various lines for the monoclinic arsenic telluride reported and those experimentally observed for our sample are presented in Table-1. Almost all the strong lines of our sample are matching to those reported for the monoclinic structure. The compound is thus identified as monoclinic arsenic telluride.

For the sample heated on glass plates at 150°C, the electron diffraction pattern showed spots on the diffraction lines with d = 3.10 and 1.52 Å in the plane of incidence. This is indicative of a partial orientation of some planes parallel to the glass substrate. Due to overlapping of several reflections it is not clear which plane is parallel to the substrate but it appears likely that it could be $20\bar{1}$ or 112.

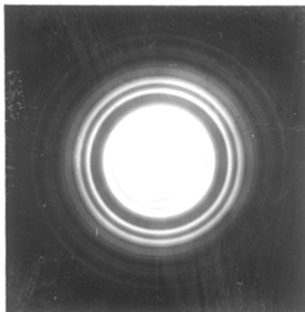

Fig.5. Electron diffraction patterns, by transmission (above) and by reflection (below) of As_2Te_3 thin film.

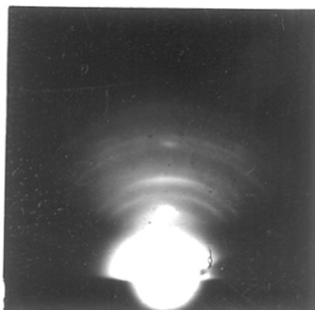

<u>Table-1</u>

	Reported Transmission		Observed Transmission		Observed Reflection
hkl	d (Å)	Relative intensity	d (Å)	Relative intensity	d (Å)
1	2	3	4	5	6
200	7.14	W.	6.85	W.	
201	5.55	W.	5.48	W.	
$20\bar{2}$	4.23	W.			
$11\bar{1}$ 400	3.62 3.57	W.	3.78	M.S.	
003 401	3.28 3.27	S.	3.25	M.S.	
$11\bar{2}$ 310 $40\bar{2}$ 112 $31\bar{1}$	3.07 3.06 3.02 3.00 2.97	V.S.	3.05	S.	3.10
203 311	2.89 2.88	W.			
402	2.88	V.W.			
312 $11\bar{3}$ $40\bar{3}$	2.54 2.53 2.53	M.			

1	2	3	4	5	6
510 403 $31\bar{3}$ $51\bar{1}$	2.33 2.32 2.31 2.30	S.	2.32	B.S.	2.38
204 601	2.29 2.28	M.			
511 $60\bar{2}$	2.23 2.22	V.W.			
313 $51\bar{2}$	2.18 2.16	W.			
602 114 512	2.07 2.05 2.05	M.	2.10	B.S.	2.07
020	2.00	M.	1.99	M.	1.94
$31\bar{4}$ 005 $51\bar{3}$ 021	1.97 1.97 1.96 1.96	M.S.			
513	1.84	W.	1.85	W.	
710 $71\bar{1}$ $22\bar{2}$	1.82 1.81 1.81	M.			
800 $80\bar{1}$	1.79 1.78	W.			1.77

1	2	3	4	5	6
51$\bar{4}$	1.75	W.	1.75	W.	
115	1.74	W.			
023	1.71	W.	1.71	V.W.	
421	1.71				
42$\bar{2}$	1.67				
405	1.66	M.			
712	1.66				
514	1.63				
80$\underline{2}$	1.63				
20$\bar{6}$	1.63	M			
80$\bar{3}$	1.63				
422	1.62				
80$\bar{4}$	1.51				
621	1.50	M.	1.52	W.	1.52
224	1.50				
406	1.44				
911	1.44	M.	1.44	W.	
622	1.44				
60$\bar{6}$	1.41				
007	1.41	V.W.			1.41
02$\underline{5}$	1.40				
20$\bar{7}$	1.40				
71$\bar{5}$	1.39 }	V.W.			
804	1.39 }				
207	1.36				
10,0,$\underline{3}$	1.35	W.			
40$\bar{7}$	1.35				

1	2	3	4	5	6
$82\underline{0}$	1.33				
$82\bar{1}$	1.33	W.			
$11\bar{7}$	1.33				
$91\underline{3}$	1.31				
$31\bar{7}$	1.31	W.	1.31	W.	1.30
606	1.30				
330	1.29				
$13\underline{2}$	1.28	M.			
$33\bar{1}$	1.28				
$82\underline{2}$	1.27				
$22\bar{6}$	1.26	M.	1.25	W.	
$80\bar{6}$	1.26				
$82\bar{3}$	1.26				
$11,1,\bar{1}$	1.24				
332	1.24	W.			
11,1,0	1.24				

Thickness measurements

Thickness of the chemically deposited arsenic telluride films was found to vary with experimental parameters, such as rate of generation of gas, exposure time etc. The film thickness calculated for different runs was in the range 1200 to 1500 Å.

I-V Characteristics

The I-V characteristic, as observed on the oscilloscope using the set-up described in Fig.3b was invariably linear upto atleast 30 volts. The dc I-V characteristic as measured using the set-up described in Fig.3c was however different. The I-V plot was a straight line upto an applied voltage of ~ 5 volts (i.e. a field of $\sim 10^5$ v/cm). Above this field, the current started rising rapidly and non-linearly with respect to the applied voltage (Fig.6). At a slightly higher voltage (~ 6.5 volts) the current fell down abruptly by a factor of 4-5.

Electrical conductivity

As presented in Fig.7 all samples exhibited a dependence of conductivity on temperature of the form

$$\sigma = \sigma_o \exp(-E_a/kT)$$

The value of thermal activation energy computed from the conductivity curves is 0.47 ev and the pre-exponential factor σ_o, $\sim 5 \times 10^3$ (ohm-cm)$^{-1}$.

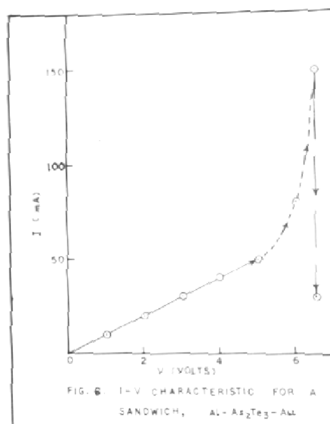

FIG. 6. I–V CHARACTERISTIC FOR A SANDWICH, Al – As_2Te_3 – Au

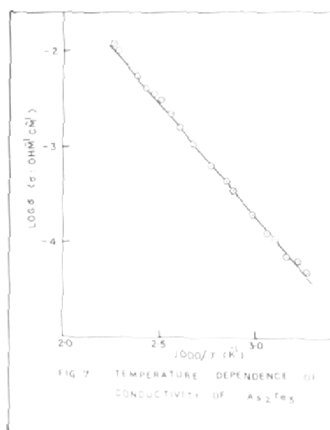

FIG. 7 TEMPERATURE DEPENDENCE OF CONDUCTIVITY OF As_2Te_3

Optical absorption

The coefficient of absorption was of the order $10^4 cm^{-1}$ at room temperature. Only $(\alpha h\nu)^2$ - $h\nu$ plot gave a good straight line which on extrapolation met the energy axis at photon energy 1.10 ev. The value of the optical band gap is taken to be 1.10 ev (Fig.8).

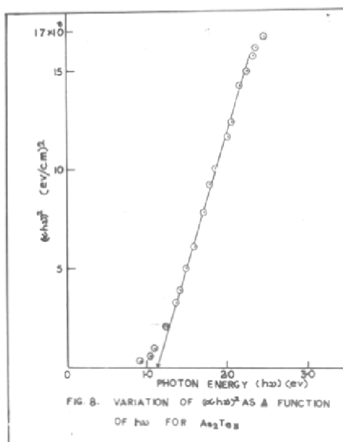

FIG. 8. VARIATION OF $(\alpha h\nu)^2$ AS A FUNCTION OF $h\nu$ FOR As_2Te_3

1.4 Discussion

There have been several earlier studies on arsenic telluride but all of them appear to deal with amorphous arsenic telluride. To the best of our knowledge we have for the first time studied the crystalline arsenic telluride in thin film form. A comparison of these two systems appears interesting.

J.M.Marshall et al.[31] have reported an inverse dependence of activation energy of noncrystalline As_2Te_3 on applied field. D.Barsen reported the increase in the activation energy with annealing temperature which he attributed to the possible crystallization taking place at high tem perature ($\sim 112^oC$); on going from amorphous to crystalline form the activation energy increases. N.Croitoru et al. reported different values of activation energies at different fields and within different temperature ranges. He concluded that over a large temperature range and at high electric fields the current was limited with space charge with a shallow trap.

Our samples were polycrystalline and showed no such dependence on annealing. The samples were taken several times

through a temperature cycle 30 - 110°C while measuring the electrical conductivity and the results repeated reproducibly. Similarly no field dependence of Ea was observed. We have obtained a constant value of activation energy equal to 0.47 ev which is roughly half of the optical band gap (= 1.07 ev). An activation energy close to (Eg/2) has been observed for many amorphous materials and is attributed to the pinning of Fermi level in the middle of the gap due to the existence of a large density of states in the gap. Such a large density of states in the gap however appears unlikely because our material is crystalline. It appears more likely that the composition is truly intrinsic because of the stoichiometry achieved in our method of preparation. The film As_2Te_3 was obtained by chemical reaction between the respective ions in solution and in view of the chemical affinity of As towards Te ions one can expect the reaction product to be As_2Te_3. Alternatively the activation energy may be partly associated with hopping. In that case the material could be extrinsic with the impurity level close to one of the band edges. The observed activation energy in that case would be predominantly associated with hopping.

Though ac I-V characteristic for sandwiches was ohmic the dc I-V plot showed significant departure from the ohmic behaviour with some characteristic features.

In case of dc I-V characteristic there was an abrupt rise of current at approximately 3×10^5 v/cm followed by a fall to a much smaller value. However in this process the film was not destroyed because one could repeat the cycle again. This might mean that some high conductivity filaments were formed which might take most of the current and get burnt. The rest of the sample remained unchanged so that the current fell back to a normal value.

In the crystalline film the observed value of optical band gap is ~ 1.1 ev. In case of amorphous material it has been reported to vary from 0.9 to 1.0 ev. The wide variation in the reported literature value of Eg opt. for amorphous materials possibly arises from the difficulty in locating the absorption edge from the experimental results. In some cases the plot at the absorption edge is not linear and so there is some uncertainty in extrapolation to zero absorption.

The graph of $(\alpha h\nu)^2$ vs $h\nu$ gave a straight line which on extrapolation to energy axis gave the value of optical band gap to be ~ 1.1 ev. This is in fair agreement with the results reported for crystalline As_2Te_3[44]. The high value of optical absorption coefficient together with the linear dependence of α on $(h\nu - Eg\ opt)^{\frac{1}{2}}/h\nu$ suggest that the As_2Te_3

is a direct band gap material. The close similarity between the optical absorption characteristics of amorphous and crystalline materials suggests that the absence of long range order does not disturb the absorption characteristics and that the optical properties are governed by the short range configuration.

References

1. J.H.Dessauer and H.E.Clark, "Xerography and Related Process", Focal Press, London, 1965.
2. A.C.Chen et al., Proc. 4th Intern. Conf. on Amorphous and Liquid Semiconductors, (PICALS), Ann Arbor, 1971.
3. D.E.Bradley, Brit. J. Appl. Phys., 5 (1954) 65, 96.
4. N.Goto and M.Ashikawa, J. Non-Cryst Solids, 4 (1970) 378.
5. S.R.Ovshinsky and P.H.Klose, (PICALS), Ann Arbor, 1971.
6. R.G.Neale et al., Electronics, 43 (1970) 56.
7. J.Feinleile et al., Appl. Phys. letters, 18 (1971) 254.
8. J.Feinleile et al., (PICALS), Ann Arbor,1971.
9. J.F.DeWald et al., J. Electrochem. Soc., 109 (1962) 243C.
10. A.Jensen, German Patent 1213075, 1964.
11. S.R.Ovshinsky, J. Non-Cryst. Solids, 2 (1970) 99.
12. C.Feldman, Mater. Res. Bull., 3 (1968) 95.
13. K.Antonowicz et al., Carbon, 10 (1972) 81.
14. R.G.Neale, J. Non-Cryst. Solids, 2 (1970) 558.
15. C.Popescu and N.Croitoru, (PICALS), Ann Arbor, 1971.
16. T.Kaplan and D.Adler, ibid, 1971.
17. R.Shanks, J. Non-Cryst. Solids, 2 (1970) 504.
18. T.J.Kobylarz, ibid, 2 (1970) 515.
19. D.L.Nelson, ibid, 2 (1970) 528.
20. G.R.Fleming, ibid, 2 (1970) 540.
21. B.Mathur and F.O.Arntz., (PICALS), 1971.
22. G.J.Carron, Acta Crystallographica, 16 pt5 (1963) 338.
23. S.Geller, J. Chem. Phys., 33 (1960) 676.
24. T.C.Harman et al., J. Phys. Chem. Solids, 2 (1957) 181.

25. B.T.Kolomiets, Book 'Elec. props. of chalcogenide glasses, (1959).

26. K.Weiser and M.H.Brodsky, Phys. Rev., 1 2 (1970) 791.

27. N.Croitoru et al., J. Non-Crystalline Solids, 4 1 (1970) 493.

28. H.K.Rockstad, J. Non-Cryst Solids, 2 1 (1970) 192.

29. A.Hrubý and L.Štourač, Mat. Res. Bull., 6 (1971) 465.

30. H.K.Rockstad, J. Non-Crystalline Solids, 8-10 (1972) 621.

31. J.M.Marshall et al., ibid, 8-10 (1972) 760.

32. L.Štourač et al., ibid, 8-10 (1972) 353.

33. A.Abrahám, Czech. J. Phys., B 22 (1972) 1168.

34. D.Brasen, J. Non-Crystalline Solids, 11 2 (1972) 131.

35. K.Weiser, A.J.Grant and T.D.Moustakas, Private Publication, 1973.

36. J.W.Mellor, 'Comprehensive treatise on inorganic and theoretical chemistry' 9 (1933) 238.

37. C.Brauer, 'Handbook of preparative inorganic chemistry' 1 (1963) 438.

38. N.Irving, 'Dangerous properties of industrial materials' (1968) 825.

39. R.W.Berry, P.M.Hall and M.T.Harris, 'Thin film technology' (1968) 171 (D Van Nostrand Co., inc., N.J. Princeton).

40. C.Kittle, 'Elementary Solid State Physics', (1962) 109.

41. R.H.Bube, 'Photoconductivity of Solids' (1960) Chapter 7, pages 212 and 224 (Jon Wiley and Sons, Inc.).

42. Le Comber and Mort, "Electronic and Structural Properties of Amorphous Semiconductors" (1973) Chapter 2 page 56 (Academic Press, London).

43. G.R.Harrison et al., 'Practical Spectroscopy', (1949) Chapter 14, pages 363 and 369 (Blackie & Son Ltd.London).

44. J.Black et al., J. Phys. Chem. Solids, 2 (1957) 240.

CHAPTER - 2.

ARSENIC SELENIDE

2.1 Historical background

Although the compound arsenic triselenide (As_2Se_3) has been very extensively studied for the last decade, relatively very little amount of work has been done in the other region of As-Se system; in particular on arsenic tetraselenide (As_4Se_4).

Arsenic tetraselenide (As_4Se_4)

A.L.Renninger[1] found the unit cell of arsenic tetraselenide to be monoclinic and the space group $P2_1/c$. The lattice parameters are

$a = 6.69 \pm 0.01$ Å, $b = 13.86 \pm 0.02$ Å,
$c = 10.00 \pm 0.01$ A, $\beta = 113.2 \pm 0.07^\circ$.

There are four molecules per unit cell.

The atomic positions are

$\pm(x, y, z)$; $(-x, \frac{1}{2}+y, \frac{1}{2}-z)$ and $(x, \frac{1}{2}-y, \frac{1}{2}+z)$ with the atomic positional parameters as given below.

	x	y	z
As (1)	0.3595	0.0185	0.1088
As (2)	0.5627	-0.1420	0.4337
As (3)	0.1718	-0.1293	0.3325
As (4)	0.3380	-0.1528	0.0364
Se (1)	0.6601	0.0077	0.3374
Se (2)	0.0930	0.0240	0.2130
Se (3)	0.6080	-0.2250	0.2450
Se (4)	0.0670	-0.2150	0.1150

J.J.Bastow et al.[2] also reported the unit cell for arsenic tetraselenide to be monoclinic but the space group was given as $P2_1/n$. The lattice parameters are also different from those reported by A.L.Renninger.

$a = 9.63 \pm 0.02$ Å, $b = 13.80 \pm 0.04$ Å,

$c = 6.73 \pm 0.02$ Å, $\beta = 107 \pm 0.5^{\circ}$.

Atomic positions are

	x	y	z
As (1)	0.1141 (4)	0.0182 (3)	-0.2452 (8)
As (2)	0.4271 (4)	-0.1405 (3)	-0.1367 (8)
As (3)	0.3256 (4)	-0.1312 (3)	0.1752 (8)
As (4)	0.0363 (4)	-0.1603 (3)	-0.2962 (9)
Se (1)	0.3485 (4)	0.0101 (3)	-0.3065 (8)
Se (2)	0.2132 (4)	0.0252 (3)	0.1245 (8)
Se (3)	0.2414 (4)	-0.2323 (3)	-0.3729 (9)
Se (4)	0.1018 (5)	-0.2178 (3)	0.0526 (9)

E.J. Samail et al.[3] and P.Goldstein and A.Paton[4] have also reported crystal structure data on As_4Se_4 on similar lines.

G.M.Orlova[5] studied the optical properties, photoconductivity and electrical conductivity of vitreous $AsSe_x$ compositions ($0.8 \leqslant x \leqslant 2.5$). The variations in the amount of Se had only a slight effect on the photoconductivity and on the optical properties but there was a considerable effect on the electrical conductivity, the density, hardness and other physical properties. The electrical conduction had a maximum at x = 1.5.

Kazuo Arai et al.[6] compared the electrical properties of Ag doped and undoped As-Se system. The dependence of dc conductivity on temperature in both the cases obeyed the exponential law:

$$\sigma = \sigma_o \exp(-Ea/kT)$$

The variation of $\sigma_{300^\circ K}$ and Ea with the composition of As-Se system had a maximum and minimum respectively at the stoichiometric composition As_2Se_3. The value of Ea for 1%Ag doped As_4Se_4 was ~ 0.76 ev whereas for As_4Se_4 it was ~ 0.96 ev.

Arsenic triselenide (As_2Se_3)

The structural, electrical, optical and photoconducting properties of arsenic triselenide (As_2Se_3) in the form of single crystal, polycrystalline material, vitreous bulk material and thin films have been studied in detail. The compound has a monoclinic structure[7]. Its dc conductivity showed intrinsic behaviour giving rise to an activation energy of conduction equal to 0.9 ev. The band gap Eg was found to be approximately 1.8 ev[8] for the amorphous and glassy systems and 2.10 ev for polycrystalline and single crystalline samples. Temperature dependence of mobility was found to be exponential which indicated an activated transition of the carriers for the shallow traps in the band. It was also

found that at low temperatures, the conductivity of amorphous As_2Se_3 was much less than that of the crystal which was attributed to the influence of dangling bonds and to some extent also to impurities.

The ac conductivity[9] was found to be proportional to w^n with $n = 0.95 \pm 0.05$ in frequency range 1.0×10^2 to 5.0×10^7 Hz. Different models for frequency dependent conduction have been considered. The thermally activated hopping has been concluded to be the most likely process. At low temperatures, ac conductivity of amorphous As_2Se_3 nearly independent of temperature but strongly dependent on the frequency[10]. The frequency dependence of ac conductivity was linear upto 10^6 Hz and quadratic in the range 10^6 to 10^8 Hz. Above 10^8 Hz the conductivity was not dependent on frequency. This suggested that the ac conductivity of the amorphous As_2Se_3 could not be interpreted by the hopping conduction alone and the effects of spatial inhomogeniety might have a role in the conduction mechanism.

Photoconductivity and light absorption studies on amorphous thin films[11] of As_2Se_3 gave the optical band gap as 1.77 ev and for single crystals between 2.03 and 2.26 ev[12]. The value reported for glassy As_2Se_3 was $\sim$ 1.85 ev[13]. The dependence of the square root of absorption coefficient on

photon energy gave two rectilinear portions intersecting the energy axis at 0.21 and 0.56 ev.

H.J.De Wit and C.Crevecoeur[14] studied the I-V characteristic of As_2Se_3 glass as a function of thickness and temperature of the specimen. They found that a deviation in Ohm's law started at 1.6×10^5 v/cm at room temperature. Evaporated In, Al and Au were used as the electrodes. A third grounded guard electrode served to drain off surface currents. They claimed that the observed deviation was not caused by self-heating.

A.E.Owen and T.M.Roberston[15] discussed in detail the dc and ac conductivity, thermoelectric power, optical absorption and carrier mobility of As_2Se_3. They concluded that though the ac conductivity involved hopping, the dc properties were best reviewed in terms of a band model with a "mobility gap" as introduced by Mott and Cohen. AC conductivity problems have not yet been resolved. A.E.Owen[16] also studied electronic conduction mechanism in Ag doped As_2Se_3 and concluded that basically a band model is appropriate for As_2Se_3, modified by tail of the localized states.

A.V.Danvilov et al.[17] studied the electrical conductivity in the vitreous system $AsSe_{1.5} - Cu_x$. The conductivity was found to increase with Cu concentration.

The plot of log (Eg) vs -log(Cu) increased linearly in the region of x from 0.6 to 0.16. It was also found that at 19 at % Cu the band gap Eg reduced to 0.87 from 1.83 ev for pure As_2Se_3. The effect of 5 to 8 at % of Be, Mg, Ca, Zn caused a change in conductivity at 20°C by less than a factor of 10.

A.V.Danvilov and collaborators[18] studied the effects of Cu and Ag on photoelectric properties of As_2Se_3. As the Cu or Ag content was increased, the maximum and the red edge of the photoconductivity were found to be displaced towards the long wavelength region. The results were in good agreement with the data obtained from the temperature dependence of electrical conductivity of the same compositions. It was also deduced that the solubility of Cu in As_2Se_3 is approximately three times as large the solubility of Ag and that Cu reduces the forbidden band width more strongly. The high solubility of Cu was attributed to the fact that the effective radii of Cu, As and Se are similar (1.28, 1.25 and 1.16 Å respectively) and to the high capacity of Cu for forming coordinate valence bonds which impede crystallization of glass.

B.T.Kolomiets et al.[19-20] have made similar studies (in the dopant range 0-2.4 at·% Cu or Ag) and their results are in general agreement with the above findings. They have also tried Ga, In and Tl as dopants and observed a similar behaviour in regard to the effect of impurities on conductivity, activation energy and shift in spectral response. A study of kinetics of photoconductivity for all the glass compositions showed the existence of traps for the majority and minority carriers in the band gap.

2.2. Crystalline Arsenic tetraselenide (As_4Se_4 thin films)

2.2.1. Experimental techniques

Preparation of thin films of arsenic selenide

Thin films of arsenic selenide were prepared by the action of hydrogen selenide on an aqueous solution of arsenic trichloride solution by the following method. These films were subsequently identified to be As_4Se_4.

An aqueous solution of arsenic trichloride was prepared as described in the previous chapter. The required basic compounds, Al_2Se_3 and FeSe, for the preparation of hydrogen selenide[21] gas were prepared by melting the stoichiometric mixture of the required elements in evacuated quartz capsules. Here iron selenide is preferred to aluminium selenide because the latter is highly unstable in moist air and so more dangerous to handle than FeSe.

The whole experimental set-up was installed exactly on similar lines as described earlier in case of arsenic telluride. The only change made was that the aluminium telluride was replaced by iron selenide in order to get hydrogen selenide gas. The subsequent experimental procedure was repeated on exactly similar lines as described earlier to obtain arsenic selenide film. The film so obtained was

washed thoroughly and picked up on glass substrates, dried and preserved in a desiccator for further measurements.

Arsenic trichloride solution with concentration range 0.01 - 0.02 M and pH range 2-4 gave good results. The compound FeSe used here for the preparation of H_2Se, was freshly prepared and preserved under dry conditions.

2.2.2. Results

Electron diffraction

Fig.1 displays the transmission electron diffraction pattern for a specimen of arsenic selenide film.

The experimentally observed 'd' values and relative intensities for our sample are presented in Table-1 together with the calculated values of 'd' for monoclinic As_4Se_4 using

$a = 6.69$ Å, $b = 13.86$ Å,

$c = 10.0$ Å, $\beta = 113.2^{\circ}$.

The agreement is reasonably good.

Table-1

Observed			Calculated
hkl	Relative intensity	d (Å)	d (Å)
11$\bar{3}$	V.S.	3.27	3.22
33$\bar{1}$	S.	1.98	1.98
110	S.	1.70	1.77
114	W.	1.39	1.39
027	M.	1.29	1.29
511	M.	1.16	1.15
512	W.	1.09	1.08

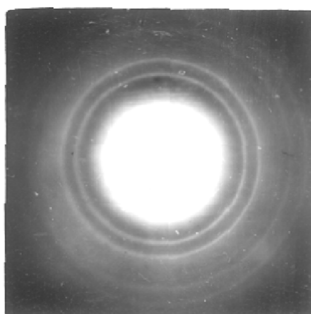

Fig.1. Electron diffraction pattern (transmission) of As_4Se_4 thin film.

Our 'd' values do not match to any other reported As-Se compound except As_4Se_4. Thus the compound is identified as arsenic tetraselenide.

Thickness measurements

Thickness of the chemically deposited thin films of crystalline As_4Se_4 was found to vary with experimental conditions. Thickness of the films used for the electrical and optical measurements was in the range 1800-2000 Å.

I-V Characteristics

In case of dynamic I-V characteristics, a straight line passing through origin was obtained upto an applied voltage of 20 volts ($\sim 10^6$ v/cm).

In case of dc I-V characteristic an ohmic behaviour was observed upto applied voltage $\sim$ 5 volts (10^5 v/cm). At this voltage there was an abrupt increase in current ($\sim$400 mA) followed by a sudden fall ($\sim$ 40 mA) (Fig.2). This behaviour is similar to that obtained for As_2Te_3.

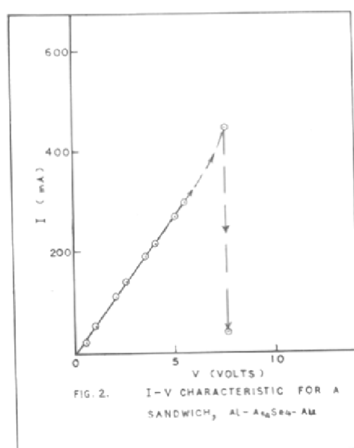

FIG. 2. I–V CHARACTERISTIC FOR A SANDWICH, Al – As_4Se_4 – Au

Electrical conductivity

The plot of log σ - 1/T for chemically deposited crystalline films showed two slopes. The low temperature slope was found to correspond to an activation energy 0.15 ev whereas the value on high temperature side was 0.92 ev. The extrapolated values for the pre-exponential factors were of the order $\sim 10^{-3}$ and 10^{6} (ohm-cm)$^{-1}$ for the two linear portions respectively (Fig.3).

Optical absorption

For our sample only $(\alpha h\nu)^2$ - $h\nu$ plot gave a fairly good straight line. On extrapolation, the graph intersected the energy axis at photon energy $\sim$ 1.95 ev (Fig.4).

When we attempted to compare the results on these films of As_4Se_4, it turned out there were no measurements reported on the electrical, optical and transport properties of bulk As_4Se_4. The only study published so far on As_4Se_4 is related to the synthesis and crystal structure. We therefore undertook the work on the electrical properties of bulk As_4Se_4. We attempted to prepare single crystal and vitreous states of the compound and study the bulk properties.

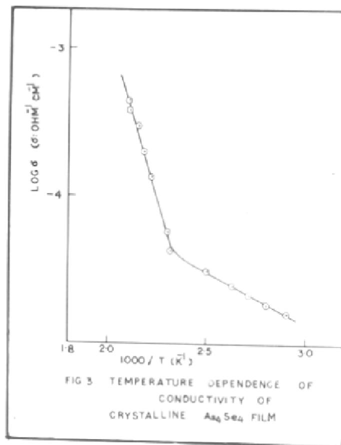

FIG 3 TEMPERATURE DEPENDENCE OF CONDUCTIVITY OF CRYSTALLINE As_4Se_4 FILM

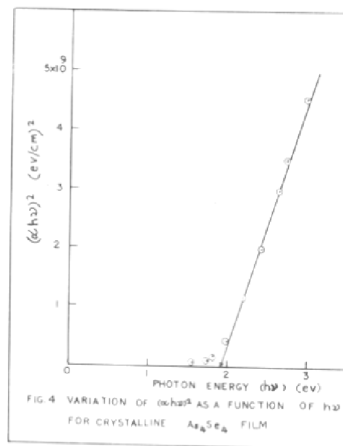

FIG 4 VARIATION OF $(\alpha h\nu)^2$ AS A FUNCTION OF $h\nu$ FOR CRYSTALLINE As_4Se_4 FILM

Unfortunately our preliminary attempts to grow large sized crystals from melt have been unsuccessful. Further attempts are being made, the results will be published elsewhere.

Here we are reporting on the bulk properties of vitreous As_4Se_4 with several dopants. In addition to this evaporated thin films of As_4Se_4 (amorphous) have also been studied. The experimental techniques along with the results are presented in the following pages.

2.3. Amorphous As_4Se_4 (bulk)

2.3.1. Introduction

It is wellknown that the formation of sharp band edges in crystals is a consequence of periodicity. Although long range order is unlikely in non-crystalline systems, the existence of short range order in these amorphous or glassy materials has been detected by radial distribution function studies. Over a few interatomic distances the peaks observed for amorphous material are almost identical to those for corresponding crystalline material. This is the reason why amorphous or glassy materials are expected to maintain some sort of a band structure with possibly diffused band edges.

Like crystalline materials the electrical properties of majority of amorphous semiconductors are found to be dependent on the previous history of the compound such as the method of preparation, consequent thermal treatments etc. Crystalline semiconductors are known to be very much sensitive to impurities, on the other hand non-crystalline materials are much less sensitive to impurities. In crystalline semiconductors each impurity

atom is forced by a long range order to have the co-ordination number of the host atom it substitutes whereas in amorphous materials each atom can satisfy its own valence bonds by adjusting its nearest neighbour environment.

It is commonly found for amorphous semiconductors that the slope of the plot log σ -1/T gives a value of activation energy approximately equal to half of the optical band gap of the amorphous compound. (The values of the optical band gap for amorphous and crystalline state of the same compound are quite comparable). In addition, such materials appear to remain 'intrinsic' even with the incorporation of small amounts of foreign impurities. The Hall effect also remains intrinsic at low temperatures for most of the amorphous compounds. These observations suggest that the Fermi level is close to the center of the gap as is observed in the intrinsic crystalline semiconductors, free from gap states ($n=p$). But there is an evidence of the existence of large number of holes and electrons in localized tail states and gap states of amorphous materials showing $n \neq p$.

Regardless the type of conduction whether p or n - type, thermoelectric power measurements also suggest that Fermi level is close to the gap center. The above findings led to the conclusion that the Fermi level is pinned near the center of the gap because of the existence of gap states. Amorphous germanium however is an exception where $Ea \neq \frac{1}{2}$ Eg opt. The value of activation energy at room temperature is reported to be 0.15 ev whereas the optical band gap for crystalline Ge is 0.7 ev.

The concept of mobility shoulder or edge is introduced by N.F.Mott[22]. It is regarded as the sharp energy change separating the localized state energies from the extended state energies. For value of E above the mobility edge conduction can occur without thermal activation and for values below the mobility edge an electron can move only by exchanging energy with phonons and the motion is thermally activated.

The mobility of hopping conduction between these localized states is about 10^3 times smaller than that in bands which also indicates that the conduction is phonon assisted. This is further confirmed by the experimental findings that a plot of log σ-1/T shows a change in slope at the point where the conduction via non-localized states

changes to the conduction via localized states. These localized states act as trapping centers which have been verified by the drift mobility measurements.

The optical band gap is obtained by the high absorption region involving optical interband transitions ($\alpha \geqslant 10^4$ cm^{-1}). The onset of this interband absorption curve is characterized by strong absorption, in contrast to low absorption in crystalline Ge or Si, and absorption coefficient ranges from 1 to 10^4 cm^{-1}. The general selection rules and k-conservation are no longer applicable. The absorption coefficient α, increases exponentially as

$$\alpha = \text{const} \exp h\nu/E_1 \quad \ldots\ldots\ldots\ldots\ldots\ldots \quad (1)$$

The slope E_1 lies between 0.05 and 0.08 ev for almost all amorphous semiconductors. The reason is not yet clear. The exponential absorption tail is called as Urbach tail or edge which is attributed to the band edge exciton absorption. This Urbach tail is caused by a dissociation of excitons by internal fields present in these materials[23]. These fields are estimated to be of the order 10^5v/cm. E_1 in the above expression (1) is proportional to the magnitude of the internal fields.

The portion below the edge absorption is structure sensitive and apparently associated with the absorption involving localized gap states.

According to Anderson, Mott and Cohen[24] the states become localized near the top and bottom of the band when their density falls below about 10^{21} $ev^{-1}cm^{-3}$. The lack of long range order gives rise to the tail states whereas the gap states are believed to be orginating from dangling bonds, impurities and other defects in or deviations from the random network structure. Several models have been proposed on the distribution of density states[25-28]. However the estimation of the upper limit to the density of gap states by various methods such as field effect, screening length and tunnelling experiments do not tally with results obtained from optical absorption.

2.3.2. Experimental techniques and results

Preparation of vitreous arsenic tetraselenide (As_4Se_4 bulk)

The starting materials, arsenic and selenium, used for the preparation of the compound, were of 4 N purity. These materials were further purified by sublimation in evacuated quartz capsules to 10^{-6} mm Hg. In case of arsenic the charge was held at 600-620°C whereas selenium was sublimed at 300-320°C. These initially purified materials were mixed in appropriate proportions in an agate mortar and transferred to a quartz capsule which was then evacuated to 10^{-6} mm Hg and sealed. This sealed quartz capsule containing the charge was heated slowly to 400°C and held at that temperature for one day. The temperature was then raised slowly to 800°C and the capsule was held at this temperature for six days. The capsule was intermitently shaken to ensure a thorough mixing and removal of voids in the bulk material. After the 6th day the capsule containing the melt was water quenched and the ingot of vitreous As_4Se_4 was obtained. Thin slices of size $\sim$ 0.1 cm x 0.7 cm x 0.6 cm. were cut out from the ingot for the electrical conductivity measurements.

Six different samples were prepared with six different dopants viz. Ag, Cu, Cd, Zn, Sn and Ge, taking one gram of the parent glass (As_4Se_4) and mixing 20 mg of a dopant with it (i.e. dopant concentration 2%). The reaction mixture was then heated in evacuated (10^{-6} mm Hg) quartz capsules, with intermitent shaking, in temperature range 700-750°C for 6-8 hours and then it was water quenched. Samples of the desired shapes were cut out from the ingots for the electrical conductivity measurements.

Thin films of the parent glass (As_4Se_4) were also obtained by vacuum evaporation on glass plates and sodium chloride plates for electrical conductivity and optical measurements. The vacuum deposition unit used for our purpose is depicted in the Fig.5a. It was a all glass unit consisting of a mercury diffusion pump preceeded by a rotary oil pump for fore vacuum. This vacuum unit could be operated to low pressures, of the order 10^{-6} Torr. The McLeod gauge was connected to this system to measure the inside pressure. The actual deposition of the compound As_4Se_4 or of gold and aluminium as electrodes, was done in a special chamber fitted with two standard vacuum joints B-45 and B-29 cone joints.

The B-45 cone joint connected to the vacuum line whereas the B-29 was fitted to a socket joint;B-29 carrying two electrical leads. The material to be evaporated was

Fig.5. Vacuum deposition unit.

embedded in silica wool which was placed on a helical tungsten filament. In case of gold or aluminium deposition the loops were made of the respective metal wire and allowed to hang on the filament. Before deposition the filament was cleaned by heating it to glow red hot. The distance between the source and the substrate was always 5.00 cms. The deposition was done by resistive heating of the tungsten filament (coil diameter 5.0 mm and wire diameter 0.5 mm).

X-ray powder diffraction

The bulk arsenic tetraselenide was finely ground and filled in a fine capillary, required for x-ray diffraction. Diffraction patterns were taken with Cu $K\alpha$ radiation.

Fig.6 displays the x-ray diffraction pattern for the powdered arsenic tetraselenide. Only broad haloes were noticed indicating the vitreous nature of the compound.

Size and thickness measurements

In case of vacuum deposited thin film of amorphous As_4Se_4, thickness was measured by the usual multiple beam interferometery method.

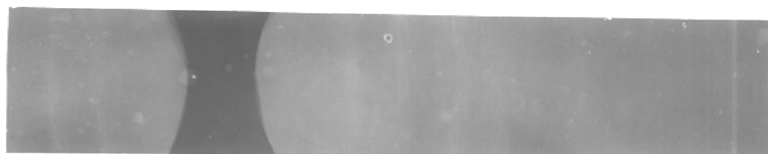

Fig.6. X-ray diffraction pattern of As_4Se_4 .

The sizes of the slices cut out of the glassy ingot of As_4Se_4 were precisely measured with the help of a micrometer screw guage.

Thickness of the evaporated thin films of As_4Se_4 was found to vary with evaporation conditions. The thickness of the film used for the electrical and optical measurements was 1500 Å.

DTA/DTG/TG measurements

The instrument used for the measurement was 'Derivatograph' type OD-102. It measures simultaneously the change in weight (TG), the rate of change in weight (DTG), the heat content change (DTA) of the test specimen while the furnace is being heated at a nearly uniform rate.

The amount of sample (As_4Se_4 or mixture of As and Se) and of inert reference (Al_2O_3) was the same i.e. 200 mg. The reaction chamber was evacuated using a water-suction pump. The heating rate was adjusted at $10^{\circ}C$ per minute.

The DTG-galvanometer measured the current induced by the coil suspended from the analytical balance beam and moving in a magnetic field.

The DTA-galvanometer measured the difference between the voltages of two thermocouples; one from inert sample and the other from the sample under study.

The T-Galvanometer measured the temperature of the sample alone.

Fig.7a and Fig.7b display the DTA/DTG/TG curves for the reacted compound (As_4Se_4) and the unreacted mixture of As and Se of the same composition respectively.

As indicated in Fig.7a the DTA curve for arsenic tetraselenide compound has a broad exothermic peak between temperatures 90 and 320°C. From this it is interpreted that the compound started softening from 90°C and melted completely at 320°C. Another exothermic peak is observed between 460 and 600°C with a peak at 560°C whereas at the same temperatures a trough is noticed on the DTG curve. This is attributed to the evaporation of the compound. This can further be confirmed by TG curve showing a gradual loss in weight started from 460°C onwards; followed by a subsequent rapid loss from 560°C onwards. At 800°C there was total loss in weight leaving behind empty crucible.

The DTA curve presented in Fig.7b for the mixture of As and Se shows small but sharp peak at 210°C indicating the

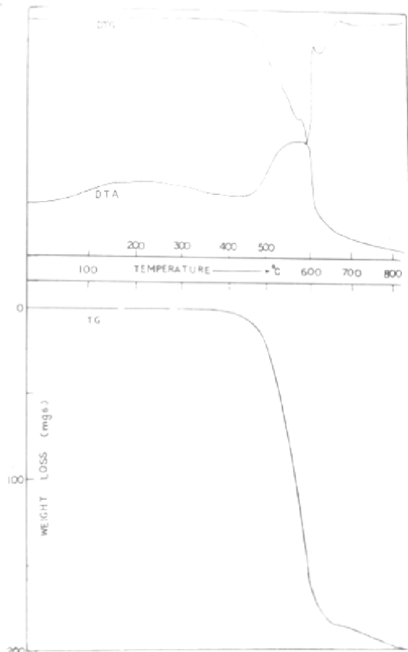

FIG.7a DTA, DTG & TG CURVES FOR As_2Se_3 COMPOUND

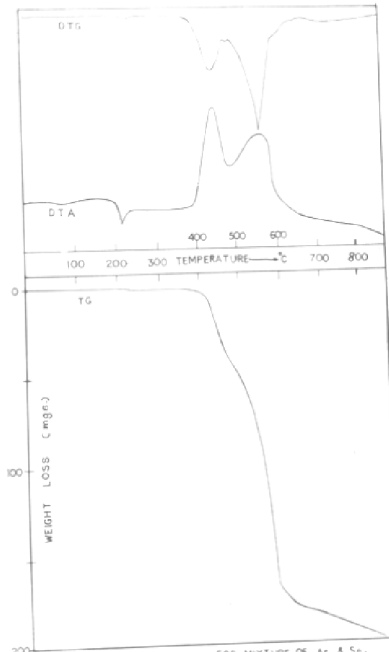

FIG.7b DTG, DTA & TG CURVES FOR MIXTURE OF As & Se.

probable incomplete reaction between arsenic and selenium taking place. The subsequent two exothermic peaks in the range 380 to 600°C indicate the evaporation of unreacted constituents and reacted compound from the parent mixture. The corresponding troughs on DTG curve can be noticed in the same temperature range. The TG curve shows a loss in weight started at 380°C followed by a rapid loss from 560°C onwards. At 800°C no residue is left behind.

As the features observed in Fig.7b (DTA, TG for a mixture of As and Se) are completely absent in Fig.7a it is concluded that no unreacted As or Se was present in the reacted compound and that a single phased compound corresponding to the composition As_4Se_4 was formed.

DC conductivity

In case of thin film of As_4Se_4 the usual two point arrangement was used with evaporated gold electrodes.

The thin slices cut out of the bulk material were given gold electrodes at the two opposite faces so as to sandwich the slice in between the gold electrodes. The slice was then placed on a gold foil inside the sample holder. Pressure contacts were given with the help of phosphor bronze strips to the gold foil as well as to the top electrode.

Using the conductivity cell described earlier the dc conductivity was measured.

The conductivity graphs for the 8 samples, i.e. As_4Se_4(thin film), As_4Se_4(bulk), As_4Se_4 + 2% Ag, As_4Se_4 + 2% Cu, As_4Se_4 + 2% Cd, As_4Se_4 + 2% Zn, As_4Se_4 + 2% Ge and As_4Se_4 + 2% Sn are illustrated serially in 8 to 15 figures.

In the case of samples of As_4Se_4(thin film), As_4Se_4 + 2% Ag and As_4Se_4 + 2% Cu a plot of log σ - 1/T gave two distinct slopes. The activation energies Ea_1 and Ea_2 depicted in the Table-1 correspond to the slopes on low and high temperature sides respectively.

In case of samples, As_4Se_4(bulk), As_4Se_4 + 2% Cd, As_4Se_4 + 2% Zn, As_4Se_4 + 2% Sn and As_4Se_4 + 2% Ge conductivity was almost constant with increasing temperature in the range 300 to 400°K. Thereafter it was found to increase exponentially with temperature obeying the relation

$$\sigma = \sigma o \exp(-Ea_2/kT)$$

where Ea_2 is the activation energy corresponding to the higher temperature side slope of the respective graph.

The numerical values of activation energies (Ea) and pre-exponential factors (σo) from the respective plots

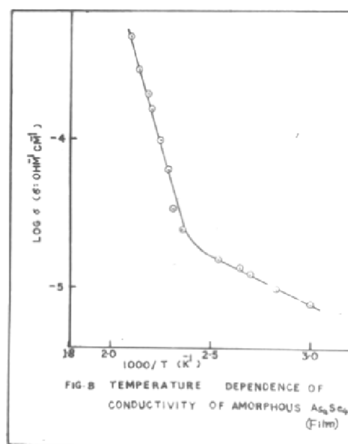

FIG. 8 TEMPERATURE DEPENDENCE OF CONDUCTIVITY OF AMORPHOUS As_4Se_4 (Film)

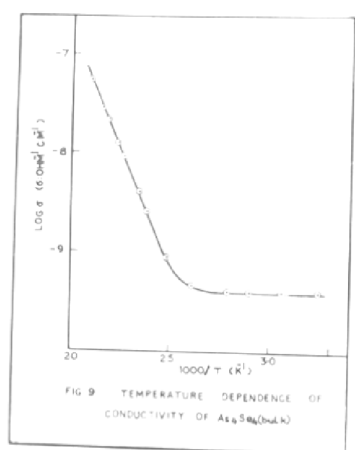

FIG. 9 TEMPERATURE DEPENDENCE OF CONDUCTIVITY OF As_4Se_4 (bulk)

FIG. 10 TEMPERATURE DEPENDENCE OF CONDUCTIVITY OF Ag-DOPED As_4Se_4 (bulk)

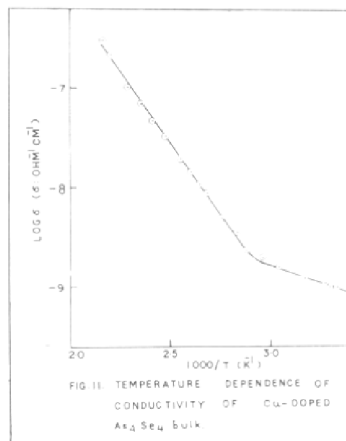

FIG. 11. TEMPERATURE DEPENDENCE OF CONDUCTIVITY OF Cu-DOPED As_4Se_4 bulk.

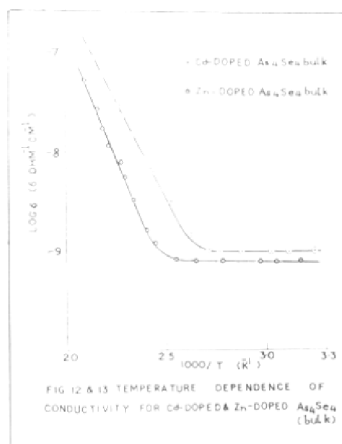

FIG. 12 & 13. TEMPERATURE DEPENDENCE OF CONDUCTIVITY FOR Cd-DOPED & Zn-DOPED As_4Se_4 (bulk)

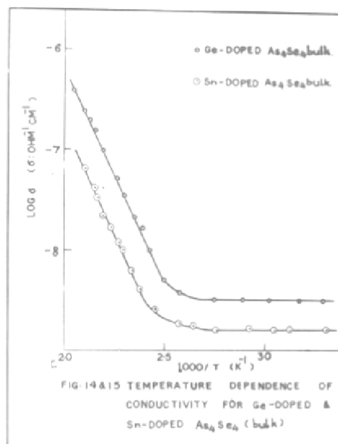

FIG. 14 & 15. TEMPERATURE DEPENDENCE OF CONDUCTIVITY FOR Ge-DOPED & Sn-DOPED As_4Se_4 (bulk)

of log σ-1/T for different samples are given in Table-1.

Table-1

Fig. No.	Compound	Activation energy ev Ea_1	Ea_2	Pre-exponential factor σ_0 $ohm^{-1}cm^{-1}$
8.	As_4Se_4(thin film)	0.13		9.5×10^{-3}
			0.94	1.7×10^{7}
9.	As_4Se_4(bulk)	0.00		4.0×10^{-10}
			0.99	447.0
10.	As_4Se_4 + 2% Ag	0.20		7.9×10^{-6}
			0.55	0.3162
11.	As_4Se_4 + 2% Cu	0.13		2.8×10^{-7}
			0.58	0.6310
12.	As_4Se_4 + 2% Cd	0.00		1.0×10^{-9}
			0.80	31.60
13.	As_4Se_4 + 2% Zn	0.00		7.9×10^{-10}
			0.95	1.6×10^{3}
14.	As_4Se_4 + 2% Ge	0.00		3.2×10^{-9}
			0.90	3.2×10^{2}
15.	As_4Se_4 + 2% Sn	0.00		1.6×10^{-9}
			0.90	1.8×10^{2}

Optical absorption

Arsenic tetraselenide was vacuum deposited on a glass substrate. The absorption spectrum of the deposited thin film was scanned in the visible range on a ratio recording Beckmann spectrophotometer. Absorption coefficient, α, was calculated on similar lines as explained in the first chapter. The graphs, α^2 vs $h\nu$, $\sqrt{\alpha}$ vs $h\nu$, $\sqrt{\alpha h\nu}$-$h\nu$, log α-$h\nu$ and $(\alpha h\nu)^2$ - $h\nu$ were plotted.

Absorption coefficient, α, for the vacuum deposited thin film (1500 Å) of As_4Se_4 was in the range 10^3 to $10^4 cm^{-1}$ at room temperature. A plot of $(\alpha h\nu)^2$ vs $h\nu$ is depicted in Fig.16. The straight line when extrapolated intersected the energy axis at 2.00 ev (= Eg opt). The plot $(\alpha h\nu)^2$-$h\nu$ gave a better straight line compared to any other plot, therefore the value 2.00 ev was taken as the direct band gap for the material.

Arsenic tetraselenide was vacuum deposited on sodium chloride ir windows, in order to check its transparency to ir region. Thicker deposits, about few microns, giving dark red colour were used for the measurements. The spectrum was scanned on Perkin Elmer model 212, in the frequency range 600 to 3700 cm^{-1}. Thickness of the deposited film was calculated with the help of the

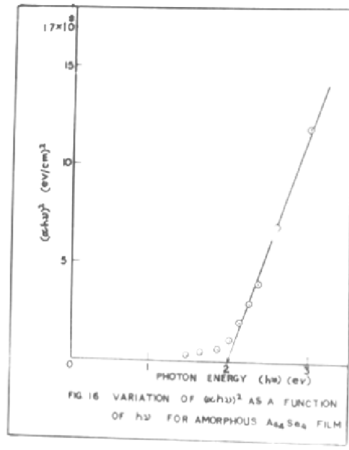

FIG 16 VARIATION OF $(\alpha h\nu)^2$ AS A FUNCTION OF $h\nu$ FOR AMORPHOUS As_4Se_4 FILM

fringes obtained on the ir spectrum. The formula used :

$$nt = \frac{N}{2(\nu_1 - \nu_2)}$$

where t : true spacing

: thickness of the film

N : number of fringes

ν_1 and ν_2 : frequencies between which the fringes are counted.

n : Refractive Index of As_4Se_4 (unknown)

The thick film of As_4Se_4 deposited on sodium chloride substrate showed a complete transparency to ir region ranging from 600 to 3700 cm^{-1} (Fig.17). The thickness of the deposited film calculated from the fringes obtained on ir spectrum was $\frac{10.53}{n}\mu$(micron). The value of refractive index of As_4Se_4 is not available in literature; the value is yet to be determined.

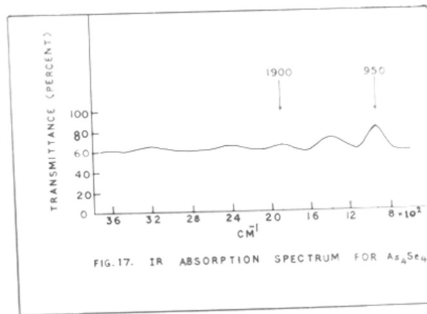

FIG. 17. IR ABSORPTION SPECTRUM FOR As_4Se_4

2.4 Discussion

The compound As_4Se_4 can be made crystalline, glassy or amorphous depending on the method of preparation. In amorphous or glassy semiconductors there is no evidence for shallow donors near the conduction band or shallow acceptors near the valence band. Here each atom can satisfy its valence bonds by adjusting its nearest neighbour environment, on the other hand in crystalline semiconductors each impurity atom is forced by long range order to have the co-ordination number of the host atom it substitutes. Impurity effect in amorphous materials is lessened because of the presence of gap states and pinning of E_f due to impurities. There is no evidence of shallow donors or acceptors controlling the conductivity at low temperature.

So far there is no electrical or optical studies made on As_4Se_4. The films prepared by chemical deposition were crystalline. The log σ - 1/T plot gave two values for activation energies. Low temperature activation energy equal to 0.15 ev and high temperature 0.95 ev. This suggests an impurity level near the band edges must have been formed. The compound was not intentionally doped. Impurity level might be arising from nonstoichiometry. The compound As_2Se_3 is reported to undergo photodecomposition[29] and this

process is further promoted by the presence of moisture. Our crystalline films were prepared by chemical reaction in water medium in presence of light. However after drying, the films were preserved in a black paint coated desiccator to stop the further reaction. The photodecomposition in moist air is described by the reaction :-

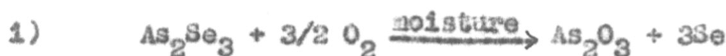

i) $As_2Se_3 + 3/2\ O_2 \xrightarrow{\text{moisture}} As_2O_3 + 3Se$

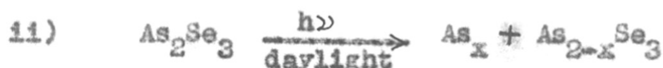

ii) $As_2Se_3 \xrightarrow[\text{daylight}]{h\nu} As_x + As_{2-x}Se_3$

Our compound might undergo similar reaction as

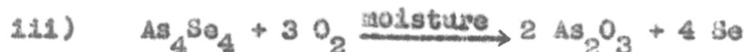

iii) $As_4Se_4 + 3\ O_2 \xrightarrow{\text{moisture}} 2\ As_2O_3 + 4\ Se$

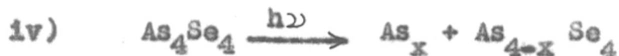

iv) $As_4Se_4 \xrightarrow{h\nu} As_x + As_{4-x}\ Se_4$

$0 < x < 4$

Non-stoichiometry developed from the above possible reactions may be responsible for the creation of impurity level at 0.15 ev. In case of vacuum deposited films the possible thermal decomposition and possible formation of molecules like - As_2Se_2, $AsSe_4$, As_4Se_2, AsSe, As and Se as reported by R.F.Shaw[12] may be responsible to create an impurity level at 0.13 ev. High temperature activation energy in both crystalline and amorphous films is comparable and can be attributed to the intrinsic conduction as $Ea = \frac{1}{2}Eg$.

The above possibilities of extrinsic conduction have been ruled out in case of bulk As_4Se_4 glass where only one conductivity slope corresponding to an activation energy 0.98 ev is observed. This value is roughly one half of the optical band gap (=2.0 ev) suggesting the intrinsic conduction.

Two per cent doping of Cd or Zn, Sn or Ge found to have no effect on electrical conduction of glassy As_4Se_4.

2% doping of Ag or Cu in As_4Se_4 bulk glass showed pronounced effect on conductivity. Both Ag and Cu gave two slopes corresponding to low and high activation energies. In neither case intrinsic region was attained upto 120°C at which the glass started softening. K.Arai et al.[6] reported the temperature dependence of electrical conductivity of Ag doped As-Se glass with a single activation energy. They observed a decrease in the activation energy with increase in Ag concentration, and concluded that the effect of Ag on the conductivity is related to the ratio of Se to As in the parent glass. They have interpreted their results on the basis of mobility of the impurity. Formation of a compound Ag_2Se is favoured in Se rich As-Se system without cutting many bonds between As and Se and Ag impurity under such conditions considered to be less mobile. On the other hand in As rich

glass, formation of Ag_2Se may cause many cuttings of As-Se bond leaving 'As' free. 'Ag' surrounded by such As-defects was considered to be more mobile. They have considered Ag and Cu to be mobile impurities in As-Se system, affecting the electrical conduction to the considerable extent. These authors have not clarified why only Ag or Cu affect the electrical conduction and other impurities have no such effect.

B.T.Kolomiets et al.[30] and others[31-35] also studied the effect of impurities on the conductivity and photoelectric properties of glassy As_2Se_3. The observed initial decrease of conductivity, with Ag and Cu upto 0.2 at.% was attributed to the increase in carrier scattering introduced by impurities or by lattice imperfections caused by them. Further increase in the concentration of these impurities caused a decrease of activation energy and was attributed to a possible transition to a more ordered structure since mobility was increased. They concluded that these impurities in glassy As_2Se_3 reduce the depth of trapping centres for majority and minority current carriers in the band gap.

The As-Se system is reported as p-type since holes are the major current carriers[10]. The observed low and high values of activation energies which we have obtained can be explained on the basis of two types of impurity states.

The carriers originating from the low lying impurity states (close to the valence band) start contributing to conduction process at low temperatures. If the density of states in these impurity levels is small then at high temperature the carriers originating from the deeper levels where the density of states is presumably higher, overtake and predominate the conduction process. This conduction corresponds to the high activation energy.

In both the cases, crystalline and amorphous As_4Se_4 the relation

$$\alpha = C\,(h\nu - Eg\ opt)^{\frac{1}{2}}/h\nu$$

holds good. The values of optical activation energy for both the states of As_4Se_4 are comparable. The values are 2.0 and 1.95 ev for amorphous and crystalline As_4Se_4 respectively. We conclude from the above results that the optical transitions in both amorphous and crystalline As_4Se_4 are direct and allowed ones.

References

1. A.L.Renninger and B.L.Averbach, Acta Cryst., B 29 (1973) 1583.

2. J.J.Bastow et al., J. Chem. Soc. Dalton Trans., 17 (1973) 1739.

3. E.J.Samail et al., Acta Crystallogr., Sect. B, 29 (Pt 9) (1973) 2014.

4. P.Goldstein and A.Paton, Acta Crystallogr., Sect. B, 30 (Pt 4) (1974) 915.

5. G.M.Orlova, Izv. Akad. Nauk. SSSR. Neorg. Mater., 4 10 (1968) 1646.

6. Kazuo Arai et al., Japan.J. Appl. Phys., 11 8 (1972) 1080.

7. A.A.Vaipolin, Soviet Phys. Crystallogr., 10 5 (1966) 509.

8. S.A.Dembovskii and A.A.Vaipolin, FTT, 6 6 (1964) 1769.

   J.T.Edmond, Brit. J. Appl. Phys., 17 (1966) 1979.

   V.I.Kruglov et al., Vestn. Leningrad Univ. Fiz. Khim., 23 (10) (1968).

   Josef Struke, Festkoerperprobleme, 9 (1969) 46.

9. A.L.Lakatos et al., Phys. Rev. B, Ser. 3, 3 6 (1971) 1791.

10. Michihiko Kotao, Japan.J. Appl. Phys., 11 10 (1972) 1472.

    R.A.Street and A.D.Yoffe, J. Non-Crystalline Solids, 8-10 (1972) 745.

11. B.T.Kolomiets and V.M.Lyubia, FTT, 4 2 (1962) 401.

    M.Kitao et al., Japan.J. Appl. Phys., 8 (1969) 499.

12. R.F.Shaw et al., J. Non-Crystalline Solids, 4 1 (1970) 29.

13. V.I.Kruglov et al., Vestn. Leningrad. Univ., 21 (16), Ser. Fiz. Khim. No.3, (1966) 66.

    Michihiko Kitao et al., Japan.J. Appl. Phys., 12 7 (1973) 1077.

14. H.J.De Wit and C.Crevecoeur, Phys. Lett., A 33 1 (1970) 25.

15. A.E.Owen and T.M.Robertson, J. Non-Crystalline Solids, 2 1 (1970) 40-51.

16. A.E.Owen, Glass Indus., 48 (11)(1967)637 and 658; 48 (12)(1967) 695 and 698.

17. A.V.Danilov et al., Zh. Prikl. Khim., 35 (1962) 2012.

18. A.V.Danilov and Collaborators, FTT, 5 (1963) 2015; 1472.

19. B.T.Kolomiets et al., J. Non-Cryst. Solids, 5 5 (1971) 389.

20. B.T.Kolomiets et al., ibid, pages 402-14.

21. G.Brauer, 'Handbook of Preparative Inorganic Chemistry' 1 (1963) 418.

22. P.G.Le Comber and J.Mort, 'Electronic and Structural Properties of Amorphous Semiconductors', (Academic Press, London) (1973) Chapter 1, P.20.

23. J.D.Dow and D. Redfield, Phys. Rev. Letts., 26 (1971) 762.

J.D.Dow and D.Redfield, Phys. Rev. Letts., B 5 (1972) 594.

24. N.F.Mott and E.A.Davis, "Electronic processes in Non-Crystalline Materials" (Clarendon press) 1971.

25. E.A.Davis and N.F.Mott, Phil. Mag., 22 (1970) 903.

26. M.H.Cohen et al., Phys. Rev. letts., 22 (1969) 1065.

27. N.F.Mott, J. Non-Cryst. Solids, 8-10 (1972) 1.

28. J.M.Marshall and A.E.Owen, Phil. Mag., 24 (1971) 1281.

29. J.S.Berkes et al., J. Appl. Phys., 42 12 (1971)4908-16.

30. B.T.Kolomiets et al., J. Non-Cryst. Solids, 5 (1971) 389.

31. A.V.Danilov et al., FTT, 5 (1963) 2015.

32. B.T.Kolomiets et al., Proc. Intern. Conf. on the Physics of Semiconductors, Exter, (1962) P.259.

33. A.M.Andriesh et al., FTT, 4 (1962) 2286.

34. B.T.Kolomiets and Yu. V. Rukhlyadev, FTT, 8 (1966) 2762.

35. V.I.Kruglov and A.I.Bobov, Vestn. Leningr. Univ., Ser. Fiz. Khim. No. 10 (1966) 125.

CHAPTER - 3.

ANTIMONY TELLURIDE

3.1. Historical background

The unit cell of Sb_2Te_3 is rhombohedral[1] and the space group is $R\bar{3}m\ D^5_{3d}$. The unit cell may be transformed to a bigger hexagonal cell, the lattice parameters for which are as follows.

$$a = 4.25 \pm 0.02\ \text{Å}, \qquad c = 30.0 \pm 0.02\ \text{Å}.$$

There are three molecules in the hexagonal unit cell.

The atomic positions are as follows.

6 Sb in 6 (c) at $0,0,Z;\ 0,0,\bar{Z}$.
with $Z = 0.400$

3 Te in 3 (a) $0,0,0$.

6 Te in 6 (c) at $0,0,Z;\ 0,0,\bar{Z}$.
with $Z = 0.211$

$$+\left\{\begin{array}{l} 0,0,0; \\ \frac{1}{3},\frac{2}{3},\frac{2}{3}; \\ \frac{2}{3},\frac{1}{3},\frac{1}{3}. \end{array}\right.$$

T.C.Harman et al.[2] studied the electrical and thermal properties of p-type Sb_2Te_3. The carrier concentration in Sb_2Te_3 was found to be approximately $7 \times 10^{19}/cm^3$ which was attributed to the high "wrong atom" defect level.

J.Black et al.[3] studied the electrical and optical properties of Sb_2Te_3 single crystals. Infra red transmission was poor presumably because of high carrier concentration. Small amount of transmission from 3.63 to about 5 microns was observed. The edge was found to correspond to an energy gap of 0.3 ev. Hall and resistivity data were taken in a range of temperatures around 300°K and the sample was found to be extrinsic.

Sh.Movlanov et al.[4] prepared zone refined single crystals of Sb_2Te_3. The electrical conductivity for the samples was found to be anisotropic and its component along the x-axis was approximately 7 times that across it. The conductivity curves showed that the minimum electrical conductivity occurred at the maximum thermal emf.

V.A.Brodovii and V.I.Lyashenko[5] also prepared single crystals and studied the temperature dependence of conductivity, Hall constant, mobility and thermal emf. They obtained ohmic contacts for Sb_2Te_3 by applying Wood's alloy and pure Pb. It was found that the concentration of the current carriers over a wide range of temperatures (from -150° to 150°C) did not depend on temperature. The mobility decreased with a rise in temperature indicating that the scattering of current carrier by thermal oscillations of the

lattice predominated. The dependence of the effective mass on temperature was calculated from the measurements of thermal emf.

N.S.Rajagopalan and S.K.Ghosh[6] measured the electrical conductivity, Hall mobility and thermoelectric power of vacuum deposited polycrystalline films of Sb_2Te_3 with aquadag electrodes. The measurements were taken before and after heat treatment. The observed large increase in conductivity and thermoelectric power after heat treatment led them to conclude that inter-crystallite barriers were present before the heat treatment. Variation of log (R) with temperature before and after heat treatment showed that the inter-crystallite barrier height reduced to one tenth of its value on heat treatment. Before heat treatment E_a = 0.05 ev and after heat treatment it fell to 0.006 ev. Mobility was found to depend on the thickness of the film and only slightly on heat treatment.

B.Rönnlund et al.[7] studied the electrical properties of doped Sb_2Te_3. Seebeck coefficient and electrical conductivity were measured on Sb_2Te_3 doped with Pb, I, $CuBr_2$, Sn etc. The material was always found to be strongly p-type with the Seebeck coefficient $S \simeq 80\ \mu V/^{o}K$. The Seebeck coefficient, S, was plotted as a function of electrical

conductivity, σ , for Sb_2Te_3 with various dopants. The S versus σ curve indicated the existence of two valence bands separated by 0.23 ev.

V.S.Tyushev and O.V.Shelud'Ko[8] studied the Hall effect, electrical conductivity and thermo-emf of evaporated Sb_2Te_3 films at 20°C. The Sb_2Te_3 films were p-type and their electrical resistivity was found to be dependent on the height of the intercrystallite barrier, h. For freshly prepared films, 'h' was equal to 0.06 ev and was found to decrease by an order of magnitude after thermal treatment at 100°C. The mobility, μ, increased with the film thickness, d, and was found to depend only slightly on 'h'. The thermoelectric power was found to depend only slightly on the evaporation velocity and on 'd' but it decreased strongly with 'h'.

I.A.Smirnov et al.[9] studied the temperature dependence of the Hall coefficient, electrical conductivity, thermoelectric power and thermal conductivity. From the data on thermal conductivity and Hall effect they concluded that Sb_2Te_3 has a complex valence band. The thermoelectric power data and Hall effect suggested that the gap between the sub-bands became narrower with increasing temperature.

C.Straub and Z.Kocsis[10] studied the specific resistance and Hall voltage of polycrystalline Sb_2Te_3 at various temperatures. The specific resistance was found to have a maximum value approximately at $400^\circ K$. Data on minority charge-carrier concentration showed that thermal scattering predominates in stoichiometric samples. The defect site concentration was found to be high in Sb_2Te_3; owing to the similarity between the ionic radii of the two constituents, which favours incorporation of foreign atoms. The temperature dependence of mobility was found to be a 3.4 - power function of temperature.

A.A.Averkin et al.[11] studied the change in the electrical properties of Sb_2Te_3 under hydrostatic pressure in order to support the supposed existence of complex structure in the valence band of Sb_2Te_3. The coefficient of thermo-emf, electrical conductivity and Hall coefficient were measured as a function of hydrostatic pressure upto 15 kbar; on p-type Sb_2Te_3 single crystals as well as on doped Sb_2Te_3 with various amounts of I, Te, Pb and Zn. Pure bismuth or Wood's metal was used for the electrodes. All the samples were found to exhibit an increase in electrical conductivity and thermoelectric power and a decrease in Hall coefficient with increasing pressure. The experimental

results were explained on the basis of two subbands of holes in antimony telluride, mutually shifted by pressure, and the strong influence of interband scattering.

K. Yokota and S. Katayama[12] studied the effects of annealing time and temperature on Seebeck coefficients of Bi_2Te_3, Bi_2Se_3 and Sb_2Te_3. For p-type Sb_2Te_3, the samples annealed at 400°C were found to show larger Seebeck coefficient than those annealed at 500°C.

3.2. Experimental techniques

Preparation of thin films of antimony telluride (Sb_2Te_3)

Thin films of antimony telluride (Sb_2Te_3) were prepared by the action of hydrogen telluride gas on an aqueous solution of antimony trichloride.

An aqueous solution of antimony trichloride ($SbCl_3$) was prepared using the method described by J.R.Glauber and P.L.Robiquet[13]. Antimony trioxide was heated in concentrated hydrochloric acid and the resulting solution was further diluted to desired concentration. Hydrolysis of antimony trichloride by water was retarded by the presence of excess hydrochloric acid and tartaric acid. The solution so prepared was then exposed to hydrogen telluride gas following the same procedure and using the same experimental set-up as described earlier.

The thin film of antimony telluride so obtained was washed thoroughly, picked up on sodium chloride and glass substrates and dried. The samples were preserved in a desiccator for further measurements.

The concentration of $SbCl_3$ was in the range 0.01 - 0.02 M while the pH range was 2-4.

The electron diffraction, thickness measurements, I-V characteristics of sandwiches such as Al-Sb_2Te_3-Au, and the electrical conductivity measurements were carried out on similar lines as described earlier.

Thermoelectric power measurements

The measurements were carried out on thin ($\sim$4000 Å) film of Sb_2Te_3 in temperature range 300 to 400°K.

Fig.1 displays the experimental set-up along with the sample holder used for the thermoelectric power measurements. A glass plate, coated with tin oxide, was used as the internal microheater. It was fixed at one end under the sample whereas at the other end an ordinary glass plate of the same thickness was inserted to balance the level. The contacts were given to the tin oxide heater, with the help of air drying solderable silver paint. The copper leads were soldered to these silver electrodes and then connected to a stabilized power supply.

A glass plate bearing Sb_2Te_3 film was then placed on this microheater. The gold electrodes were previously deposited one centimeter apart on the Sb_2Te_3 film. Two copper-constantan thermocouples were fixed on both the gold electrodes with the help of thermally conducting but electrically insulating paste. These two different thermocouples read two end-temperatures separately on the

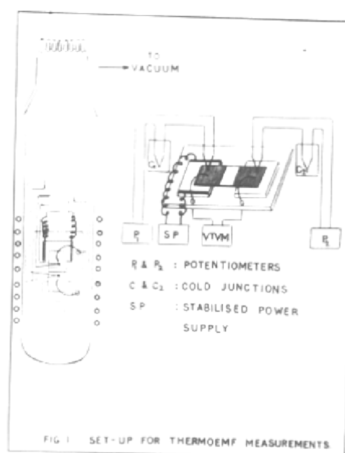

FIG 1 SET-UP FOR THERMOEMF MEASUREMENTS

potentiometer.

Two press contacts were given to two gold electrodes with the help of phosphor bronze strips. These strips were connected to a vacuum tube voltameter to record the thermoemf. The sample holder assembly was placed in a vertical tubular furnace which acted as an external heating source. Measurements were carried out under vacuum ($\sim 10^{-3}$ Torr).

Optical absorption

The thin ($\sim$4000 Å) film of Sb_2Te_3 was taken on a sodium chloride ir window, dried carefully in a vacuum desiccator. The absorption spectrum for the dried film was taken on a Perkin Elmer Model-137 IR Spectrophotometer in region from 3 to 5 microns. The graphs of $(\alpha h\nu)^2$-$h\nu$ and $(\alpha h\nu)^{\frac{1}{2}}$-$h\nu$ were plotted.

3.3. Results

Electron diffraction

Fig.2 displays the transmission electron diffraction pattern for a sample of antimony telluride film.

The 'd' values and relative intensities for the various lines for rhombohedral Sb_2Te_3, for our sample are given in Table-1 along with the reported 'd' values[14].

Table-1

	Reported	Observed	
hkl	d (Å)	d (Å)	Relative intensity
101	3.17	3.14	S.
102	2.37	2.31	V.W.
110	2.11	2.12	M.
201	1.84	1.76	W.
202	1.54	1.57	V.W.
212	1.36	1.37	W.
300	1.24	1.24	V.W.

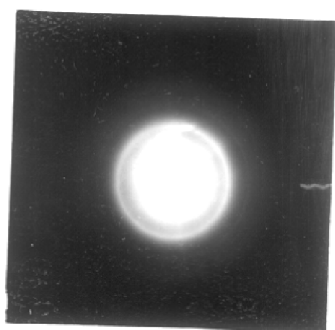

Electrical properties (I-V characteristics, DC conductivity and Thermoelectric power)

In case of dynamic I-V characteristic the sandwich Al-Sb_2Te_3-Au showed an ohmic behaviour upto applied field 10^6 v/cm ($\sim$20 volts).

In case of dc I-V characteristic there was an abrupt increase of current (140 mA) with subsequent drop ($\sim$30 mA) at an applied field 10^5 v/cm. The plots, I vs V and log I vs V were not straight lines bu the plot log I vs log V (Fig.3) gave a good straight line with a slope equal to 2.

The thickness of the films used for the measurements of electrical conductivity was found to be $\sim$4000 Å.

The plot of log σ- 1/T for a thin film of Sb_2Te_3 in the temperature range 300 to 400°K gave a straight line with a constant slope. The heating and subsequent cooling of the same sample gave fairly reproducible results and a constant value of activation energy equal to 0.12 ev was obtained (Fig.4).

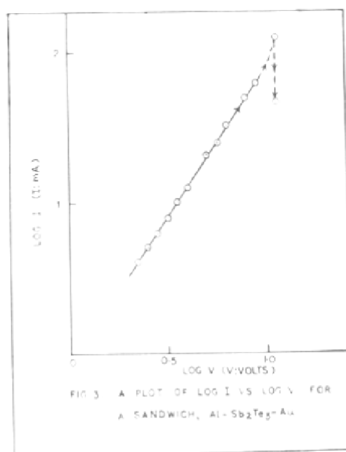

FIG. 3 A PLOT OF LOG I VS LOG V FOR A SANDWICH, $Al-Sb_2Te_3-Au$

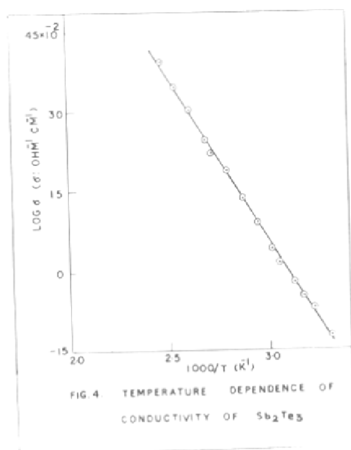

FIG. 4 TEMPERATURE DEPENDENCE OF CONDUCTIVITY OF Sb_2Te_3

The films studied here were from the same lot from which the samples selected for dc conductivity. Temperature gradient was varied from 5° to $20^{\circ}C$ setting the two heaters in different ways. Seebeck coefficient calculated from the readings was of the order $\simeq 50 \pm 20 \mu V/^{\circ}K$ and was found to be independent of temperature (Fig.5).

Optical absorption

Absorption coefficient, α, for a thin ($\sim$4000 Å) film of Sb_2Te_3 was of the order $10^4 cm^{-1}$ at room temperature. A plot of $(\alpha h \nu)^2$ vs $h\nu$ is illustrated in Fig.6. The value of the optical band gap obtained from the extrapolation of the graph is ~ 0.27 ev (Eg opt).

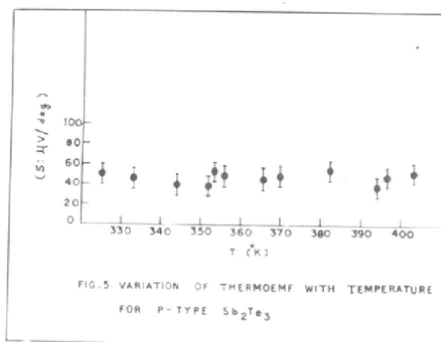

FIG. 5. VARIATION OF THERMOEMF WITH TEMPERATURE FOR P-TYPE Sb_2Te_3

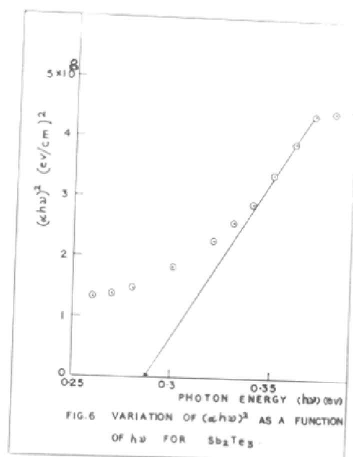

FIG. 6 VARIATION OF $(\alpha h\nu)^2$ AS A FUNCTION OF $h\nu$ FOR Sb_2Te_3

3.4. Discussion

It was not possible for the previous investigators to derive the energy gap Eg between valence and conduction bands from the electrical measurements since the intrinsic region started at about 610°C only 15° below the melting point of Sb_2Te_3. Metallographic investigations proved that it is not possible to prepare the stoichiometric compound Sb_2Te_3. It always gives two phases namely the eutectic of SbTe enriched in Te, and Te. Sb replaces Te^1 sites to give Sb rich compound as

The thermo-emf measurements of our sample gave a constant value of Seebeck coefficient, S, equal to $50 \pm 20 \mu V/^{\circ}K$ which gives an approximate value of the energy difference between the valence band edge and the Fermi level equal to 0.015 ev whereas the activation energy computed from the conductivity slope is 0.12 ev. The higher value of activation energy by about ~ 0.10 ev obtained in the conductivity slope suggests that the extra activation energy may be associated with mobility. Two carrier transport will give low value of S for intrinsic semiconductors. This could be a possible explanation but is considered less likely because the hole mobility and density are known to be much

higher than those of electrons. If the material was amorphous one could have thought this as the possibility but for a crystalline Sb_2Te_3, this looks unlikely in view of several previous reports on this material.

The activation energy roughly matches to the half of the band gap which may tempt one to suggest that the material was intrinsic. It may behave like an intrinsic semiconductor if the Fermi level is pinned at somewhere in the middle of the gap due to the existence of a large number of states.

However this is considered unlikely in view of our thermoelectric power data. The material appears to be extrinsic. The material was not intentionaly doped and it is likely that excess of Sb is responsible for the extrinsic conduction. The extra activation energy appeares to be associated with mobility as in case of hopping semiconductor. In single crystals the predominant scattering mechanism is due to phonon. It is reported that the concentration of the current carriers was independent of temperature whereas the mobility was found to decrease with a rise in temperature. Our experimental value of activation energy associated with mobility can be expressed by the relation,

$$\mu = \mu_0 \exp\left(-\frac{\Delta E}{kT}\right) \quad \text{where } \Delta E = 0.12 \text{ ev.}$$

The exponential increase of mobility with temperature observed in our sample is in agreement with the results reported earlier[10].

The reported measurements on thin film revealed that the mobility increases appreciably with the thickness of the film but the effect of heat treatment and of the height of intercrystallite barrier was insignificant.

The Seebeck coefficient S, for the thin films was reported to depend only slightly on film thickness but found to decrease very strongly on the intercrystallite barrier or grain boundaries. Our films showed no sifnificant change in Seebeck coefficient even after annealing. Fairly constant value of S, suggested that our samples were free from grain boundaries.

A plot of log I vs log V is a straight line with a slope equal to 2 (Fig.3). This indicates the conduction mechanism is space-charge-limited and the traps are distributed uniformly.

Metal insulator ohmic contact obeys Ohm's law at low fields as long as the injected carrier density is lower than the thermally generated free carrier density. When the former predominates a space charge builds up at the electrodes.

The generated current is termed as space charge limited current (SCLC). Mott and Gurney[15] deduced the following expression for (SCLC) density J;

$$J = 10^{-13} \mu \epsilon \frac{V^2}{d^3}$$

where

d = thickness of the insulator along the direction of the field

μ = Mobility of the charge carriers

ϵ = dielectric constant of the insulator

V = applied potential in volts

The above relation holds good for trap free process. Existence of traps causes a large fraction of the injection space charge to condense therein with consequent reduction in the free carrier density. Filling of traps is a temperature dependent process. R.W.Smith and A.Rose[16], M.A.Lampert[17] suggested temperature correction for an insulator with shallow traps as

$$J \propto \mu \epsilon \theta \frac{V^2}{d^3}$$

where $\theta = N_c/N_t \exp(-E_a/kT)$

and Ea is the energy associated with the traps N_t, below the conduction band and Nc is the density of state at room temperature. When all traps are filled the further injection

of charges will obey the relation for trap free process i.e. square law dependence of I or J on voltage. J or I increases with temperature indicating the presence of shallow traps. Conduction process in our sample is thus (SCLC) with shallow traps.

Our samples showed a proper, though weak, absorption edge. Antimony telluride is a direct band gap material with optical band gap equal to 0.27 ev. There is considerable absorption even below the absorption edge. The reason is not clear but is likely to be due to gap states or excitons.

References

1. Structure Reports, 20 (1956) 36.
2. T.C.Harman et al., J. Phys. and Chem. Solids, 2 (1957) 181.
3. J.Black et al., ibid, 2 (1957) 240.
4. Sh.Movlanov et al., Doklady. Akad. Nauk. Azerbaidzhan. SSSR, 17 (1961) 375.
5. V.A.Brodovii and V.I.Lyashenko, Ukr. Fiz. Zh., 6 (1961) 664.
6. N.S.Rajagopalan and S.K.Ghosh, Physica, 29 (1963) 234.
7. B.Rönnlund et al., J. Phys. Chem. Solids, 26 (1965) 1281.
8. V.S.Tyushev and O.V.Shelud'Ko, Izv. Vyssh Ucheb. Zaved. Fiz., 10 1 (1967) 46.
9. I.A.Smirnov et al., Fiz. Tverdogo Tela, 10 6 (1968) 1782.
10. C.Straub and Z.Kocsis, Veszpremi Vegyip. Egyet. Kozlem., 11 1 (1968) 33.
11. A.A.Averkin et al., Fiz. Tverdogo Tela, 12 11 (1971) 3356.
12. K.Yokota and S.Katayama, Oyo Butsuri, 41 3 (1972) 224.
13. J.W.Mellor, 'Comprehensive treatise on inorganic and theoretical chemistry', 9 (1933) 470.
14. L.H.Gadgil, J. Vac. Sci. Tech., 6 4 (1969) 591.
15. N.F.Mott and R.W.Gurney, "Electronic processes in "Ionic Crystals", (Oxford University Press, London) 1940.
16. R.W.Smith and A.Rose, Phys. Rev., 97 (1955) 1531.
17. M.A.Lampert, Phys. Rev., 103 (1940) 168.

CHAPTER - 4.

ANTIMONY SELENIDE

4.1. Historical background

The unit cell of antimony selenide[1] is orthorhombic. The space group* is Pnma, (D^{16}_{2h}). The lattice parameters are

$a = 11.77 \pm 0.01$ Å, $b = 3.96 \pm .01$ Å,
$c = 11.62 \pm 0.01$ Å.

There are four molecules per unit cell. There are five sets of atoms, all in positions 4 (c)

$(x, \frac{1}{4}, z); (\bar{x}, \frac{3}{4}, \bar{z}); (\frac{1}{2}-x, \frac{3}{4}, \frac{1}{2}+z); (\frac{1}{2}+x, \frac{1}{4}, \frac{1}{2}-z)$.

Atomic parameters are :

	x	z
Sb (1)	0.0305	0.3280
Sb (2)	0.3522	0.3597
Se (1)	0.0534	0.8732
Se (2)	0.8698	0.5566
Se (3)	0.2132	0.1935

---

* Foot Note : The axes a, b, c have been transformed to c, a and b respectively.

F.Donald et al.[2] studied the electrical resistivity of Sb_2Se_3 as a function of weight per cent of selenium and found an increase of four orders of magnitude as the proportion changed from stoichiometric through about 0.3% excess selenium. They interpreted this effect on the basis of a model in which Sb_2Se_3 crystals were embedded in a matrix of glassy selenium. E.A.Ignat'ev and M.V.Kot[3] have further concluded that in the Sb-Se system hole conduction was predominant for both, excess of Sb and Se.

M.V.Kot and I.P.Molodyan[4] derived the energy gaps from electrical conductivity and spectral response for polycrystalline layers of Sb_2Se_3 and found the values to be 1.12 and 1.17 ev respectively. The energy gap for electrical conduction for a single crystal stoichiometric Sb_2Se_3, was 1.08 ev as reported by G.P.Zharikov[5] whereas that with 1% Sb excess gave 0.91 ev and polycrystalline Sb_2Se_3 with 1% Sb excess gave the value to be 1.54 ev.

K.Sh.Kocharli et al.[6] reported the electrical energy gap for p-type Sb_2Se_3 to be 1.2 ev whereas the activation energies for the impurity levels as E_1=0.017, E_2=0.18, E_3=0.30 and E_4=0.53 ev.

P.P.Brazdzhyunas and others[7] studied the photoconductivity and absorption spectra of crystalline and

amorphous layers of Sb_2Se_3. The observed decrease in the energy of optical activation with increasing temperature was attributed to a decrease in the depth of the barrier region, produced by changes in the electron-phonon interaction. Similar results were reported by M.P.Mikalkevicius[8].

J.Black et al.[9] studied the optical and electrical properties of Sb_2Se_3 single crystals. The ir transmission at 300°K gave rise to the absorption edge at 1.2 ev which shifted to 1.30 ev at 0°K. The temperature dependence of intrinsic resistivity gave a value of 1.4 ev at 0°K (i.e. thermal energy gap at 0°K). The dark resistivity of Sb_2Se_3 films was higher compared with the single crystal and polycrystalline Sb_2Se_3 as reported by B.T.Kolomiets et al.[10].

M.V.Kot and S.D.Shutov[11] concluded that the hole conduction was predominant and that the conductivity of Sb_2Se_3 single crystal was anisotropic. The values of the activation energy for the charge carriers were correspondingly $E_{\parallel} = 1.03$ ev and $E_{\perp} = 1.05$ ev. The same authors[12] later on determined the positions of the optical axes for a biaxial Sb_2Se_3 crystal. The optical activation energy for the same crystallographic direction was found

to depend on light polarization. They attributed such a dependence to the possible complex structure for the energy zones in Sb_2Se_3.

A.F.Skubenko[13] also studied the electrical and photoelectrical properties of single crystals of Sb_2Se_3 and found the maximum photocurrent in the temperature range from -110 to 120°C was at wavelength, λ = 970 mμ. The width of the forbidden gap was determined by the red boundary of the photocurrent and found to be 1.16 ev at room temperature. The photoelectrical measurements gave the value 1.18 ev for the energy gap. Further study on the crystal made by A.F.Skubenko and S.V.Laptii[14] revealed three additional peaks on the absorption curve. One was at λ = 4.55 - 2.70 μ covering three maxima at 0.28, 0.32 and 0.36 ev and the two other peaks at 2.49 and 2.24 microns corresponding to activation energies 0.50 and 0.58 ev.

B.T.Kolomiets et al.[15] reported similar results as reported earlier. They studied current carrier sign, voltage-current, light intensity-photocurrent, spectral characteristics, kinetics of the photoelectric effect, temperature dependence of photocurrent, spectral dependence of the light absorption coefficient and characteristics of discharge of layers charged with an electron beam or ions

from a corona discharge, for the amorphous layers of Sb_2Se_3.

A.Efstathiou et al.[16] studied the optical density, dark conductivity and photoconductivity of evaporated Sb_2Se_3 films as a function of deposition conditions. The initial deposits exhibited abnormal band gap energies, as high as 1.7 ev with a source operated 20 degrees below the melting point of Sb_2Se_3 (611°C). The band gap decreased monotonically with time during a long evaporation. A final constant value in the range 1.1 - 1.2 ev was obtained when the source temperature was at or above the melting point of Sb_2Se_3. The data led them to the fact that the fractionation took place of initially stoichiometric Sb_2Se_3 until the stoichiometric Sb_2Se_3 started evaporating near the melting point of the compound.

V.M.Lyubin and V.S.Maidzinskii[17] studied the space-charged-limited currents and light intensity-photocurrent characteristics for crystalline and amorphous Sb_2Se_3. On the basis of these results they refined the nature of the energy distribution for the local centers and determined its change in going from the amorphous to the crystalline state. They found an evidence for the monoenergetic local states (traps) in the forbidden band. In going from amorphous to crystalline state, the energy distribution

was found to change from a quasicontinuous exponential to a discrete distribution.

B.Grigas and M.Mikalkevicius[18] studied the influence of the pressure of selenium saturated vapour ($pSe = 10^{-11}$- 10 torr) in the ampule during the growth of Sb_2Se_3 single crystal from the gas phase, on the electrical and photoelectrical properties. The dark resistivity at 20°C (ρ_o) was found to vary with $_pSe$ from 10^3 to 10^8 ohm-cm; $\rho_o(_pSe)$ had a maximum at $_pSe = 10^{-4}$ torr. The forbidden gap at 0°K was 1.34 ev. The variation of dark conductivity with temperature provided the evidence for local levels at 0.55, 0.40, 0.30, 0.24 and 0.18 ev. The local levels at 0.28 and 0.46 ev were due to an excess of Se and Sb respectively. The temperature coefficient of the forbidden gap was evaluated to be $-(4.7-5.7) \times 10^{-4}$ev/°K. The local levels for amorphous samples, derived from thermostimulated polarization were reported by V.L.Averyanov et al.[19] to be 0.10, 0.15 - 0.18 and 0.22 - 0.25 ev. L.G.Gribnyak[20] evaluated the local levels by studying the photocurrent kinetics and the temperature dependence of dark conductivity in range 20 to 200°C. They used needle shaped crystals containing acceptor and compensating donors with concentrations of 1.9×10^{16} and $3.6 \times 10^{14} cm^{-3}$ respectively. The sample was illuminated

by monochromatic (0.99μ) rectangular light pulses with duration 5 x 10^{-3} sec. and rise time 5 x 10^{-5} sec. The activation energies obtained for the accepter levels were 0.43 and 0.29 ev.

V.V.Sobolev et al.[21] studied the edge absorption of single crystal samples with polarizations $E \parallel a$, $E \parallel b$ and $E \parallel c$ at 295 and 90°K. The absorption edge exhibited two regions, the initial flat region and the region where sharply increased absorption coefficient appeared as a function of light polarization. At lower temperature the absorption in the initial region was lower. The absorption extrema of the valence and conduction bands were situated at different points of the K-space. One of the extrema possessed three weakly split sub-bands. The direct polarization absorption edge and the reflection peak were due to optical transitions in the points where absorption extrema of the valence and conduction bands were formed.

A.O.Aliev et al.[22] studied the Hall effect and electrical conductivity of single crystals giving aquadag electrodes. The Hall effect was measured with ac during modulation of the electric and magnetic fields with 60 and 50 Hz frequency respectively. Measurements were taken from

room temperature to $435^{o}K$. The samples showed p-type conduction throughout the temperature range used whereas the electron and hole mobility were found to be 4.6 and 14.5 $cm^2/v.sec.$ respectively.

Z.Hurych et al.[23] compared the shift of the optical absorption edge with that of the photoconductive spectral response of amorphous $Sb_{1-x}Se_x$ films as a function of composition. The results were in agreement with those reported earlier. An excess of Sb or Se caused a shift towards smaller or larger activation energies, respectively. Density of states of the quasifermi level for amorphous samples was found to be atleast 10^4 times greater than those for the single crystal samples of Sb_2Se_3.

C.Wood et al.[24] studied the optical and transport properties of amorphous and crystalline antimony selenide; stoichiometric and also with Sb and Se excess. For crystalline Sb_2Se_3 the absorption edge was at 1.10 ev whereas for amorphous Sb_2Se_3 it was at 1.3 ev. The resistivity of the stoichiometric amorphous films was comparable to that of crystals. The values of the thermal activation energies computed from the slopes of the resistivity versus temperature curve were 1.0 ev for the crystal and 0.60 ev for the amorphous films. The marked similarity in properties for both the states led them to the conclusion that there was no

no extensive band tailing into the forbidden band gap as one would expect to find from a mobility gap consideration.

R.Mueller and C.Wood[25] published a paper on the preparation of amorphous thin films of controlled composition. Various evaporation techniques were discussed and their influence on the optical properties was studied. The optical energy gap was found to increase with increasing selenium content. The extrapolation of the curve square root of ($\alpha h\nu$) vs $h\nu$ for amorphous Sb_2Se_3 to $\alpha = 0$ gave a value of optical energy gap (Eg opt) to be 1.25 ev.

C.Wood et al.[26] studied the optical and transport properties as a function of composition in a complete range of Sb-Se system. The absorption edges for different compositions were found to obey the relation for non-direct transitions. A tremendous variation in energy gap from 1.9 to 0.40 ev on increasing the Sb : Se ratio was observed. Electrical conductivity of all the compositions was measured as a function of temperature and activation energies were determined from a least-squares fit to the equation :

$$\sigma = \sigma_0 \exp(-Ea/kT)$$

For the conduction in extended states 'Ea' represents the energy difference between the Fermi level (E_f) and the

majority carrier band gap edge (E_V).

Optical energy gap at room temperature and the thermal activation energy were plotted as a function of composition. A break in both the curves was noticed in the vicinity of Sb_2Se_3. At this composition 2 Ea $\simeq$ Eg opt. This led to the fact that there was a symmetrical distribution of states with the Fermi level pinned near the center of the gap. The observed results, 2Ea $>$ Eg opt at high Sb contents or 2Ea $<$ Eg opt at high Se contents were also interpreted with possible mechanisms.

4.2. Experimental techniques

Preparation of thin films of antimony triselenide (Sb_2Se_3)

Thin films of antimony triselenide were prepared by exposing an aqueous solution of antimony trichloride to the vapours of hydrogen selenide gas.

An aqueous solution of antimony trichloride (concentration range 0.01 - 0.02 M and pH range 2-4) was prepared by the method described earlier. Iron selenide was used for the preparation of hydrogen selenide gas. Following the technique described earlier, thin films of antimony triselenide were obtained on suitable substrates. The film was taken on a quartz substrate for absorption experiments. The specimens were preserved in a desiccator for further measurements.

4.3. Results

Electron diffraction

Fig.1 displays the electron diffraction pattern by transmission obtained for Sb_2Se_3 film. The broad haloes on the pattern suggest the amorphous nature of the film.

Electrical properties (I-V characteristics and dc conductivity)

The films of thickness $\sim$ 1300 Å were used for all the measurements. The sandwich structure Al-Sb_2Se_3-Au showed an ohmic behaviour upto $\sim$ 40 volts (ac voltage) but dc I-V characteristic was somewhat different as observed in case of Sb_2Te_3. There was an abrupt shooting up of current ($\sim$140 mA) at the applied voltage $\sim$ 8 volts and at the same voltage there was subsequent drop in the current ($\sim$ 30 mA). The plots I vs V and log I vs V did not give good straight line however the plot log I vs log V gave a good straight line with a slope $\sim$ 2 (Fig.2).

Temperature dependence of conductivity for all samples obeyed the relation

$$\sigma = \sigma_0 \exp(-Ea/2kT)$$

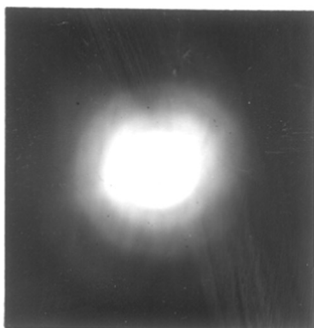

Fig.1. Electron diffraction pattern (transmission) of Sb_2Se_3 thin film.

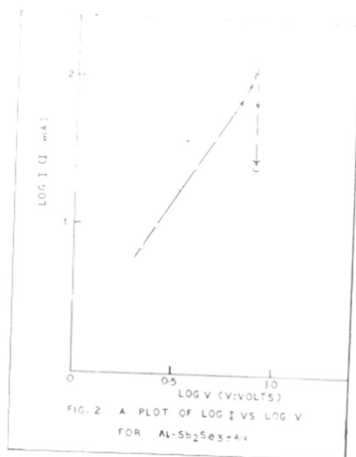

FIG. 2. A PLOT OF LOG I VS LOG V FOR $Al-Sb_2Se_3-Al$

The numerical values for Ea and σ_o computed from the conductivity curves were 0.42 ev and 31.62 $(ohm\text{-}cm)^{-1}$ respectively (Fig.3).

Optical absorption

The absorption coefficient, α, for the films was found to be of the order $10^4 cm^{-1}$ at room temperature. Out of various graphs plotted, only $(\alpha h\nu)^{\frac{1}{2}}$ - $h\nu$ gave a fairly good straight line intersecting the energy axis at photon energy 1.25 ev (Fig.4).

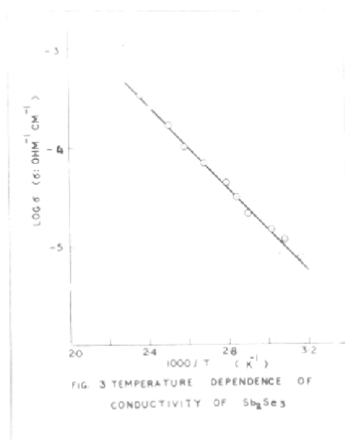

FIG. 3 TEMPERATURE DEPENDENCE OF CONDUCTIVITY OF Sb_2Se_3

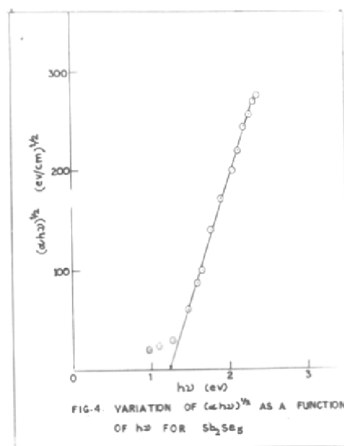

FIG. 4 VARIATION OF $(\alpha h\nu)^{1/2}$ AS A FUNCTION OF $h\nu$ FOR Sb_2Se_3

4.4. Discussion

Antimony selenide has been studied in various forms; single crystal, polycrystal or amorphous. The reported literature values for the optical band gap of the compound vary from 1.0 to 1.7 ev. Such a wide variation is attributed to the various compositions of Sb and Se. The excess of Sb causes decrease and the excess of Se causes increase in the optical activation energy.

In our sample of amorphous Sb_2Se_3 the relation

$$\alpha = \frac{C\,(h\nu - E_{g\,opt})^2}{h\nu}$$

seems to be obeyed with E_g opt = 1.25 ev. This is an indicative of indirect allowed transitions however the absorption coefficient is high, ranging from 10^3 to $10^4 cm^{-1}$. The results are in good agreement with published values[25].

The temperature dependence of electrical conductivity gave a straight line with single activation energy equal to 0.42 ev. This value is much less than half of the estimated band gap. For amorphous Ge similar results have been reported[27]. The value of activation energy for amorphous Ge was reported to be 0.15 ev at room temperature whereas the optical band gap was 0.7 ev.

Absorption below the edge is nearly zero which suggests that there are no states in the gap and no intraband absorption possible. This is interesting because amorphous material is supposed to have a large density of states in the gap. In general the relation between absorption coefficient and photon energy for amorphous materials is not simple.

The compound Sb_2Se_3 is reported to be p-type. The low thermal activation energy (0.42 ev) may be associated with impurity state at 0.42 ev above the valence band. This is not in agreement with the optical data, although past literature shows evidence of local states at the following energies 0.28, 0.32, 0.36, 0.43, 0.50 and 0.58 ev. Alternatively the Fermi level is pinned at this point due to the amorphous nature of the material. The electrical activation energy (0.42 ev) could also be due to change in mobility with temperature as in a hopper. This point could be best resolved by measuring thermo-emf or Hall effect as a function of temperature. Unfortunately we could not carry out these measurements because of the high resistance of the sample.

References

1. Wyckoff, Crystal Structures, 2 (1964) 27 and N.W.Tideswell et al., Acta Cryst., 10 (1957) 99.

2. F.Donald et al., Bull. Am. Phys. Soc., 2 1 (1956) 226.

3. F.A.Ignat'ev and M.V.Kot, Uchenye Zapiski Kishinev Univ., 24 (1956) 19.

4. M.V.Kot and I.P.Molodyan, Uch. Zap. Kish. Univ., 39 (1959) 49.

5. G.P.Zharikov, Uch. Zap. Azerbaidzhan. Gosudarst. Univ. im S.M.Kirova, Fiz. Mat. i Khim. Ser.No.3 (1960) 75.

6. K.Sh.Kocharli et al., Uch. Zap. Azverb. Gos. Univ., Ser. Fiz. Mat. Nauk 2 (1963) 83.

7. P.P.Brazdzhyunas and others, Lietuvos TSR Mokslu Akad, Darbai, Ser B, 2 (1956) 31.

8. M.P.Mikalkevicius, Elektrofotogr. i Magnitograflya, Vilnyus Sbornik, (1959) 234.

9. J.Black et al., J.Phys. Chem. Solids, 2 (1957) 240.

10. B.T.Kolomiets et al., Fiz. Tverdogo Tela, 1 (1959) 899.

11. M.V.Kot and S.D.Shutov, Uch. Zap. Kish. Univ., 39 (1959) 45.

12. M.V.Kot and S.D.Shutov, Jr. Po Fiz. Poluprovodnikov Kishinevsk, Univ., 1 (1962) 47.

13. A.F.Skubenko, Ukrain Fiz. Zhur, 6 1 (1961) 40.

14. A.F.Skubenko and S.V.Laptii, Ukr. Fiz. Zh., 9 7 (1964) 744.

15. B.T.Kolomiets et al., Magnitografiya, Vilnyus, (1965)36.

16. A.Efstathiou et al., J. Vac. Sci. Tech., 6 3 (1969) 383.

17. V.M.Lyubin and V.S.Maidzinskii, Fiz. Tekh. Poluprov., 3 11 (1969) 1702.

18. B.Grigas and M.Mikalkevicius, Liet. Fiz. Rinkinys, 9 2 (1969) 369.

19. V.L.Aver'yanov et al., Fiz. Tekh. Poluprov, 4 2 (1970) 394.

20. L.G.Gribnyak, Izv. Vyssh. Ucheb. Zaved. Fiz. 15 3 (1972) 163.

21. V.V.Sobolev et al., Issled Slozhnykh Poluprov., (1970) 183.

22. A.O.Aliev et al., Uch. Zap. Azerb., Univ. Ser., Fiz. Mat. Nauk, No.3 (1970) 72.

23. Z.Hurych et al., J. Non-Crystalline Solids, 11 2 (1972) 153.

24. C.Wood et al., J. Non-Crystalline Solids, 8-10 (1972) 209.

25. R.Mueller and C.Wood, J. Non-Crystalline Solids, 7 (1972) 301.

26. C.Wood et al., J. Non-Crystalline Solids, 12 3 (1973) 295.

27. A.H.Clark, Phy. Rev., 154 3 (1967) 750.

CHAPTER - 5.

CADMIUM TELLURIDE

5.1. Historical background

Cadmium telluride occurs in both sphalerite and wurtzite modifications depending on the method of preparation[1-2]. During its preparation by vacuum evaporation the proportion of the wurtzite form is found to increase with temperature of the substrate and also with annealing. Therefore the wurtzite is concluded to be the high temperature modification.

CdTe[3-4] : Cubic, Sphalerite, B 3 type (2), Space group $F\bar{4}3m - T_d^2$

The lattice parameter a = 6.47 Å.

There are four molecules in the unit cell and all atoms occupy special positions with coordinates

$$\left.\begin{array}{l} 4\ \text{Te in (a)}\ (0,0,0) \\ 4\ \text{Cd in (c)}\ (\tfrac{1}{4},\tfrac{1}{4},\tfrac{1}{4}) \end{array}\right\} + (0,\tfrac{1}{2},\tfrac{1}{2};\ \tfrac{1}{2},0,\tfrac{1}{2}\ \text{and}\ \tfrac{1}{2},\tfrac{1}{2},0)$$

CdTe : Hexagonal, wurtzite, B 4 type (3), Space group P6mc

The lattice parameters are

a = 4.57 Å, c = 7.48 Å.

The lattice parameters of the two modifications are related as follows :

$$a_{hex} = a_{cubic} / \sqrt{2}$$

$$c_{hex} = 2\, a_{cubic} / \sqrt{2}$$

Cadmium telluride has received a lot of attention because it can be prepared to a higher degree of purity[5] as compared to the other members of II-VI compounds and thus it offers a good scope for the study of the effect of impurity on certain fundamental properties. It is the only member which can be made highly conducting in both p- and n-type[6] which makes it accessible to a wider range of electrical measurements. For p-type CdTe the resistivity can be reached down to 0.01 ohm-cm[7] whereas for n-type down to 0.5 ohm-cm[8]. The dopant elements from groups III or VII make it n-type and those from I or V group make it p-type. The excess Cd or Te makes it n- or p-type respectively. The activation energy of conduction is about 0.003 ev for n-type and from 0.3 to 0.5 for p-type. The forbidden gap estimated from optical measurements was 1.5 ev[9].

There have been no electrical measurements of band gap. F.A.Kröger et al.[10] and D.De Notsel[6] obtained the effective mass 0.13 m for electrons and 0.41 m for holes. S.Yadama[11] compared the observed mobility with the theory of optical mode of scattering and estimated the effective mass of holes to be 0.63 m.

D.De Nobel[6] also measured Hall mobility of n-type samples as a function of temperature but discussed little on scattering mechanisms. He studied the impurity effect

in CdTe. The acceptors Ag, Cu and Au in CdTe, were found to introduce levels with an ionization energy of 0.30 to 0.35 ev. The additional level observed at 0.15 was attributed to a Cd vacancy. He observed a deeper level at 0.60 - 0.65 ev which he attributed to the doubly ionized Cd vacancy Vd^{-2}. M.R.Lorenz and B.Segall[12] have reported two other acceptor levels; one lies 0.05 ev above the valence band edge and the other 0.06 ev below the conduction band edge. He assumed these levels to be first and second ionization states of a Cd vacancy. F.Morehead and G.Mandel[8] prepared low resistivity p-type CdTe by doping with P or As but gave no data about the level depths or mobility. M.R.Lorenz and H.H.Woodbury[13] found that the nonequilibrium carrier concentration decayed as $\Delta n = \Delta n_o \exp(t/\tau)$ where τ was temperature dependent and of the form

$$\tau = \tau_o \exp(-\Delta E/kT) \text{ where}$$

$\tau_o = 3.2 \times 10^{-12}$ sec and $\Delta E = 0.27$ ev. The data indicates the carrier has to pass over a barrier of this height before recombining with the center.

There has been a considerable amount of discussion whether the minimum of the conduction band lies at k=0. The measurements[14-16] in the threshold region just below the excitation peak were interpreted in terms of a contribution

from an indirect transition. This indirect transition was found to associate with an indirect gap of the order of 0.1 ev lower than the direct gap ($\sim$ 1.5 ev). S. Yamada[17] concluded that conduction band has 4 or 8 minima along (111) axis.

The transport studies and more recent optical measurements support[18-21] the fact that the principle band edges of CdTe are at k=0 (except for the vary small shift in the position of the valence band maximum).

5.2. Experimental techniques

Preparation of thin film of cadmium telluride (CdTe)

Thin films of cadmium telluride were obtained by exposing an aqueous solution of cadmium acetate to the vapours of hydrogen telluride gas.

An aqueous solution of cadmium acetate of 0.05 M was prepared. The pH of the solution was maintained between 3-4 by adding dilute hydrochloric acid. Hydrogen telluride gas was obtained by the action of dilute hydrochloric acid on aluminium telluride. Using the experimental technique and the set-up described earlier, thin films of cadmium telluride were obtained. Film thicknesses were of the order of 1400 Å.

The electron diffraction, dc conductivity and optical absorption were studied employing the techniques described earlier.

5.3. Results

Electron diffraction studies

Fig.1 displays the electron diffraction pattern, obtained by transmission for cadmium telluride film.

The 'd' values and the relative intensities for the various lines for cubic cadmium telluride from the literature and experimentally observed 'd' values for our sample are presented in Table-1.

Table-1

hkl	Relative intensity	Observed d (Å)	Calculated* d (Å)
111	M.S.	3.72	3.73
200	W.	3.26	3.23
220	M.	2.27	2.28
222	M.	1.87	1.86
331	M.W.	1.49	1.49
422	W.	1.35	1.32
333	V.W.	1.20	1.25

* Using a = 6.50 Å.

The agreement is good, suggesting that our films are cubic cadmium telluride and since there are no extra lines

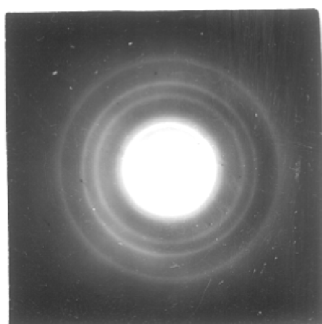

Fig.1. Electron diffraction pattern (transmission) of CdTe thin film.

it is concluded that the material is pure, homogeneous and single-phased.

DC conductivity

As illustrated in Fig.2 all four samples exhibited a dependence of conductivity on temperature of the form :

$\sigma = \sigma_o \exp(-E_a/kT)$

where $\sigma_o = 2.0 \times 10^5\ ohm^{-1}cm^{-1}$

and $E_a = 0.65$ ev

Optical absorption

Absorption coefficient for the thin (1400 Å) film of CdTe was of the order $10^4 cm^{-1}$ at room temperature. A plot of $(\alpha h\nu)^2 - h\nu$ is presented in Fig.3. The extrapolated graph intersected the energy axis at photon energy 1.6 ev (=Eg opt). The plot $\sqrt{\alpha h\nu} - h\nu$ did not give a good straight line.

The extrapolated Eg value matches with that reported for cubic CdTe.

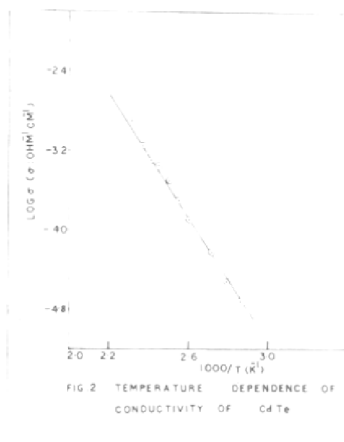

FIG 2 TEMPERATURE DEPENDENCE OF CONDUCTIVITY OF Cd Te

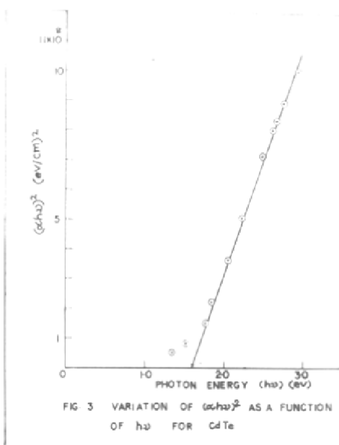

FIG 3 VARIATION OF $(\alpha h\nu)^2$ AS A FUNCTION OF $h\nu$ FOR Cd Te

5.4. Discussion

Thin films of cubic cadmium telluride can be obtained by the method of chemical deposition employed here. The vacuum evaporation is reported to give mixed phases, sphalerite and wurtzite. The latter phase increases with increasing temperature of the substrate and with rate of evaporation. However the chemical method gives a homogeneous single-phased cubic CdTe.

The activation energy obtained from log σ - 1/T curves in the temperature range 300 to 400°K was 0.65 ev. The value is roughly half the band gap of CdTe (1.6 ev). The films obtained by chemical deposition were not very highly pure so as to give an intrinsic activation energy also the range of temperature studied was much below than that required to reach intrinsic conduction. Reinhard Glang et al.[22] have reported various impurity levels arising from various dopings. Lead impurity produces p-type CdTe with a level at 0.51 ev whereas excess Te produces a level at 0.15 ev above the valence band. However we have not doped our films intentionally. B.Goldstien and L.Pensak[23] reported a level 0.6 ev above the valence band for thin films as well as for bulk p-type CdTe. They attributed the existence of this level to the impurity or crystal defect level. We suggest our films

were p-type, non-treated and showing 0.65 ev level above the valence band.

Optical absorption studies reveal that the transitions were direct and allowed. The energy of optical activation computed from the graph $(\alpha h\nu)^2 - h\nu$, was 1.6 ev.

References

1. Structure Reports, 9 (1955) 81.
2. S.A.Semiletov, Trudy. Inst. Krist. SSSR, 11 (1955) 121-123.
3. M.Aven and J.S.Prener, Phys. and Chem. of II-VI compounds, (North-Holland Publishing Company - Amsterdam.) Chapter 3 (1967) 121.
4. M.Shiojiri and E.Suito, Japan. J. Appl. Phys., 3 6 (1964) 314-319.
5. M.R.Lorenz and R.E.Halsted, J. Electrochem. Soc., 110 (1963) 343.
6. D.De Nobel, Philips Res. Repts., 14 (1959) 361.
7. B.Segall et al., Phys. Rev., 129 (1963) 2471.
8. F.Morehead and G.Mandel, Phys. lett., 10 (1964) 5.
9. N.B.Hannay, Semiconductors, (Reinhold Pub. Corp.) 1959, p.587.
10. F.A.Kröger et al., J. Electron., 2 (1955) 190.
11. S.Yadama, J. Phys. Soc. Japan, 15 (1960) 1940.
12. M.R.Lorenz and B.Segall, Phys. lett., 7 (1963) 18.
13. M.R.Lorenz and H.H.Woodbury, Phys. Rev. lett., 10 (1963) 215.
14. P.W.Davis and T.S.Strilliday, Phys. Rev., 118 (1960) 1020.
15. C.Konak, Phys. Stat. Solidi, 3 (1963) 1274.
16. W.Giriat, Acta Phys. Polon, 24 (1963) 191.
17. S.Yamada, J. Phys. Soc. Japan, 17 (1962) 645.
18. D.G.Thomas, J. Appl. Phys. Suppl., 32 (1961) 2298.
19. R.E.Halstad et al., J. Phys. Chem. Solids, 22 (1961) 109.
20. D.T.F.Marple and B.Segall, Bull. Am. Phys. Soc., 9 (1964) 223.

21. Kanazawa and Brown, Phys. Rev., 135 (1964) A 1757.

22. Reinhard Glang et al., J. Electrochem. Soc., 111 5 (1963) 407.

23. B.Goldstein and L.Pensak, J. Appl. Phys., 30 2 (1959) 155.

CHAPTER - 6.

CADMIUM SELENIDE

6.1. Historical background

Cadmium selenide occurs in both cubic and hexagonal form depending on method of preparation. It usually crystallizes in wurtzite type but during precipitation from solution at room temperature it separates out as zinc blend modification[1]. The cubic form is metastable which converts to hexagonal partially at 130° and completely on heating at 700°C for 18 hrs.[2]

CdSe : Cubic[3]

Structure type B 3, Space group $F\bar{4}3m - T_d^2$

The lattice parameter, a = 6.05 ± 0.03 Å.

There are four molecules per unit cell.

All occupy positions as explained earlier for CdTe.

CdSe : Wurtzite

Structure type B4, Space group P6mc

The lattice parameters are

a = 4.3 ± 0.01 Å,   c = 7.01 ± 0.02 Å.

There are two molecules per unit cell.

There has been very little work done on the electrical properties of cadmium selenide. D.M.Heinz and E.Banks[4] studied the Hall mobility of several n-type samples

at room temperature. The samples studied were found to have carrier concentration $3.3 \times 10^{17} cm^{-3}$ and the temperature dependence of conductivity indicated the samples were degenerate and the mobility was found to vary in the range 39 to 900 $cm^2/v.sec$.

K.Hauffe and H.G.Flint[5], Tubota et al.[6], U.Dolega[7] studied the conductivity on the partial pressure of its constituents. They found shallow donors in crystal fired under high cadmium pressure. R.Burmeizter[8] found an ionization energy of 0.014 in samples annealed under partial pressure of cadmium.

M.Itakura and H.Toyoda[9] studied heat treated CdSe in Se vapour. They found the treated crystals to be degenerate n-type with carrier concentration $3.6 \times 10^{17} cm^{-3}$ and mobility of the order 580 $cm^2/v.sec$.

D.M.Heinz and E.Banks[4], R.G.Wheeler and J.O.Dimmock[10] determined the effective mass from Zeeman splitting of excitation lines to be 0.13 m which is in good agreement with the one reported by U.Dolega[7] by studying the dependence of the thermoelectric power on carrier concentration.

S.Kubo and M.Onuki[11] measured the reflection and absorption of ir due to free carriers in n-type cadmium selenide. The optical measurements indicated that the effective masses are anisotropic. There has been no electrical measurements of the anisotropy.

6.2. Experimental techniques

Preparation of thin films of cadmium selenide

Thin films of cadmium selenide were obtained by the reaction of hydrogen selenide gas over the surface the aqueous solution of cadmium acetate.

An aqueous solution of cadmium acetage was prepared as described earlier. Hydrogen selenide gas was obtained by the action of dilute hydrochloric acid on iron selenide. Using the experimental set-up and the same procedure described earlier thin films of cadmium selenide were obtained. It was found experimentally that the concentration range 0.03 - 0.05 M and pH range $3 \sim 4$ were suitable to obtain good results.

The electron diffraction, dc conductivity and optical sbsorption in visible region were studied employing the techniques explained earlier.

Although the thickness of the films found to vary with experimental conditions, the films used for the conductivity and absorption experiments were having thickness $\sim$ 1400 Å.

6.3. Results

Electron diffraction

Fig.1 displays the electron diffraction pattern, obtained by transmission for cadmium selenide film.

The 'd' values and the relative intensities for the various line for the cubic cadmium selenide from the literature[12] and those experimentally observed for our sample are presented in Table-1. Almost all the lines of our sample are matching to those reported for the cubic structure. The compound is thus identified as cubic cadmium selenide.

Table-1

	Reported		Observed	
hkl	d (Å)	Relative intensity	d (Å)	Relative intensity
111	3.57	S.	3.50	S.
220	2.14	S.	2.12	S.
311	1.82	S.	1.80	S.
331	1.36	W.	1.37	W.
422	1.23	W.	1.19	W.
440	1.06	V.W.	1.09	V.W.

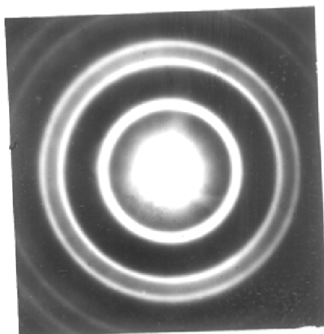

Fig.1. Electron diffraction pattern (transmission) of CdSe thin film.

DC conductivity

As illustrated in Fig.2 all samples exhibited an exponential dependence of conductivity on temperature of the form :

$$\sigma = \sigma_o \exp(-E_a/kT)$$

The value of pre-exponential factor, $\sigma_o = 25.12$ $ohm^{-1}cm^{-1}$ whereas $E_a = 0.24$ ev.

Optical absorption

Only $(\alpha h\nu)^2 - h\nu$ plot gave a good straight line. The absorption coefficient was of the order $\sim 10^4 cm^{-1}$ at room temperature. The optical band gap obtained from the graph was 1.75 ev (Fig.3).

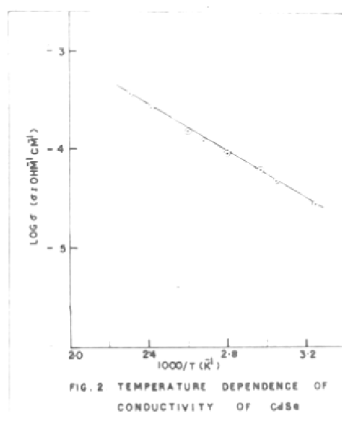

FIG. 2 TEMPERATURE DEPENDENCE OF CONDUCTIVITY OF CdSe

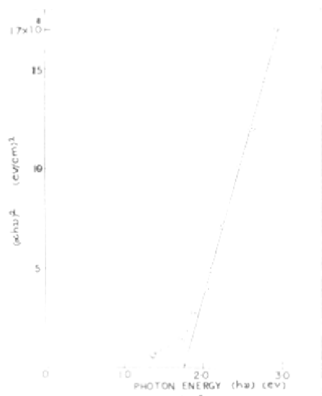

FIG. 3 VARIATION OF $(\alpha h\nu)^2$ AS A FUNCTION OF $h\nu$ FOR CdSe

6.4. Discussion

The chemical method of preparation of thin films employed here gave pure cubic phase of CdSe. The films obtained by other conventional methods were reported to contain both phases[13], cubic and hexagonal unless some special precautions[14-16] were taken; such as rate of deposition, substrate temperature etc. The existence of mixed phases in CdSe films is responsible to produce intercrystallite boundaries. The depletion layers as proposed by H.Berger[17] and R.L.Petriz[18] at such boundaries act as potential barriers for the conduction of electrons and consequently affect the electrical properties. Therefore it is essential to define the conditions of preparation and any subsequent thermal treatment of the specimen while considering the electrical properties of CdSe.

H.Berger et al.[19] studied the dependence of electron concentration on temperature and noticed the existence of two temperature regions for non-treated and annealed films at 400 and 700°C. The usual impurity conduction was observed upto 400°K. The magnitude of electron concentration and its activation energy was strongly dependent on the deposition conditions. They concluded that upto 400°C intrinsic impurities (native crystal imperfections) were effective

above all as donors in case of n-type CdSe. However above 400°C they observed a stronger dependence of electron concentration on temperature with Ea equal to 1.0 ev. From dark conductivity measurements R.H.Bube[20] and L.A.Barton determined the shallow (.14 ev) and deep (0.6 ev) donors as the different ionization states of the same crystal imperfection (anion vacancy). The shallow (0.6 ev) and the deep (1.0 ev) acceptor levels obtained from room temperature ir spectrum studies were explained as the cation vacancies with two trapped holes and one trapped hole respectively. They reported various activation energies ranging from 0.8 to 0.4 ev for CdSe crystals baked at different temperatures between 200 and 400°C whereas nonannealed samples gave 0.85 ev as the activation energy. The latter value is equal to one half the optical band gap of CdSe (viz. 1.70 ev). The crystals baked at 500°C gave single activation energy equal to 0.14 ev. Kazuo Shimizu[21] reported two donor levels, 0.14 and 0.37 ev, arising from the Se vacancies for the CdSe films baked at 100 and 150°C respectively.

Our films of CdSe were non-treated and gave a single activation energy 0.24 ev in the temperature range 300 to 400°K. The small value of activation energy suggests a new level introduced by native imperfections in the crystalline films such as Se vacancies or an extrinsic nature of the film.

Incorporation of foreign impurities[22-23] such as Cd, In, Sn, Pb causes a decrease in the resistivity of CdSe whereas Cu, Ag, Se substitute Cd from CdSe resulting in the increase in the resistivity. Copper[24] introduces an acceptor level at 0.6 ev whereas Cl or Ga gives rise to donor level at $\sim$ 0.03 ev. Indiffusion of oxygen[25-26] is believed to fill up the Se vacancies resulting in the increase of resistivity of CdSe.

However our films were not intentionally doped with foreign impurities. The possibility of the formation of potential barriers arising from the diphasic modification of CdSe is also ruled out because our samples were of purely cubic phase as confirmed with electron diffraction studies. According to R.H.Bube[27] the slope of log σ -1/T for an n-type material having donors partially compensated by acceptors, gives the ionization energy of donors. Our experimental value of activation energy appears to be associated with some donor resulting from selenium vacancies although the value is little higher than expected, which can be attributed to the crystal imperfections playing a large part in electron conduction mechanism at low temperatures.

The value of the optical band gap reported by different investigators[28-31] ranges from 1.74 to 1.84 ev. However the accepted value for the band gap is 1.7 ev. K.Rogge et al.[15] reported a shift of about 70 nm to longer wavelength for cubic phase as opposed to hexagonal phase of CdSe. Our absorption studies on cubic CdSe revealed that the optical transitions were direct and allowed with an optical activation energy 1.75 ev.

References

1. V.M.Goldschmidth, Naturwiss, 14 (1926) 477.

2. A.S.Pashinkin and R.A.Sapozhinkov, Kristallogrfiya, 7 (1962) 673. Soviet Phys. Cryst., 7 (1962) 501.

3. M.Aven and J.S.Praner, Phys. and Chem. of II-VI Compounds, (North-Holland Publishing Company - Amsterdam.) 1967 P 121, 132.

4. D.M.Heinz and E.Banks, J. Chem. Phys., 24 (1956) 391.

5. K.Hauffe and H.G.Flint, Ann. Physik, 15 (1955) 141.

6. Tubota et al., J. Phys. Soc. Jap., 15 (1963) 1701.

7. U.Dolega, Z.Natwrf, 18a (1963) 809.

8. R.Burmeister, Doctoral thesis, Stanford Univ., Stanford, California.

9. M.Itakura and H.Toyoda, Jap. J. Appl. Phys., 4 (1965) 560.

10. R.G.Wheeler and J.O.Dimmock, Phys. Rev., 125 (1962) 1805.

11. R.S.Kubo and M.Onuki, J. Phys. Soc. Japan, 20 (1965) 1280.

12. S.Nagata and K.Agata, J. Phys. Soc. Japan, 6 (1951) 523.

13. I.P.Kalinkin et al., F.T.T., 5 1 (1963) 124.

14. I.P.Kalinkin, Soviet Phys. Crystallogr., 8 3 (1963) 360.

15. K.Rogge et al., Physica Stat. Sol., 4 (1971) K 65.

16. F.V.Shallcross, Trans. AMIE,236 (1966) 309.

17. H.Berger, Phys. Stat. Sol., 1 (1961) 739.

18. R.L.Petritz, Phys. Rev., 104 (1956) 1508.

19. H.Berger et al., Physica Status Solidi, 33 (1969) 417.

20. R.H.Bube and L.A.Barton, J. Chem. Phys., 29, 1 (1958) 128.

21. Kazuo Shimizu, Jap. J. Appl. Phys., 4, 9 (1965) 627.

22. Hirosi Tubota, Jap. J. Appl. Phys., 2 5 (1963) 259.

23. Hirosi Tubota et al., J. Phys. Soc. Japan, 15 (1960) 1701.

24. R.H.Bube and E.L.Lind, Phys. Rev., 110 (1958) 1040.

25. S.G.Ellis, J. Phys. Chem. Solids, 29 (1968) 1139.

26. G.A.Somorjai, J. Phys. Chem. Solids, 24 (1963) 175.

27. R.H.Bube, Solid State Phys., 11 (1960) 230.

28. M.Itakura and H.Toyoda, Jap. J. Appl. Phys., 4 8 (1965) 560.

29. R.Ludeke and W.Paul, Phys. Stat. Sol., 23 (1967) 413.

30. Ray Brian, II-VI Compounds, (Pergamon Press N.Y.), (1969) 200.

31. R.H.Bube, Phys. Rev., 98 (1955) 431.

CHAPTER - 7.

SUMMARY AND CONCLUSIONS

The films of As_2Te_3, As_4Se_4, Sb_2Te_3, Sb_2Se_3, CdTe and CdSe were prepared by employing the chemical method described earlier. The electron diffraction patterns were taken for these films. As_2Te_3 and As_4Se_4 were identified as monoclinic. The film of Sb_2Te_3 gave a rhombohedral pattern. The films of both CdTe and CdSe were revealed to be cubic whereas the film of Sb_2Se_3 was amorphous showing only diffused rings on the pattern.

The compound As_4Se_4 was prepared in glassy form by melt quenching method. The x-ray diffraction pattern for the powdered As_4Se_4 showed broad haloes revealing its glassy nature. DTA, DTG and TG curves were studied for the compound As_4Se_4 as well as for the mixture of As and Se of the same composition and concluded that the compound As_4Se_4 was a single phased.

To study electrical properties of these films, Al or Au electrodes were deposited in vacuum. I-V characteristics for sandwiches like

(1) Al - As_2Te_3 - Au (2) Al - As_4Se_4 - Au

(3) Al - Sb_2Te_3 - Au (4) Al - Sb_2Se_3 - Au

were studied. The ac I-V plots were linear in all the cases but the dc ones showed different behaviour. The dc I-V plot for sandwiches (1) and (2) showed an ohmic behaviour upto certain fixed range of applied voltage. Above this critical voltage there was an abrupt rise in current followed by the subsequent fall in the current to a certain low value.

In case of sandwiches (3) and (4) the I-V plots were non-linear whereas the plots of log V versus log I were linear with a slope value equal to 2. This power law dependence was attributed to the space-charge-limited current.

The activation energy computed from the conductivity curves for crystalline As_2Te_3 films was found to be independent of the applied field unlike the amorphous As_2Te_3 films. Annealing of these crystalline films also showed no effect on activation energy. A constant value of activation energy observed for crystalline As_2Te_3 was 0.47 ev which is less than a half of the optical band gap (viz. 1.1 ev). This activation energy may be partly associated with hopping. The optical absorption studies revealed that the crystalline As_2Te_3 is a direct band gap material with the optical band gap equal to 1.10 ev.

The conductivity curves for the crystalline As_4Se_4 films as well as for vacuum deposited amorphous As_4Se_4 films showed two slopes with low temperature activation energy $\sim$ 0.15 ev and high temperature value $\sim$ 0.95 ev. The low temperature activation energy was attributed to the extrinsic nature of the compound arising from the possible photodecomposition or thermal decomposition during evaporation in vacuum. The high temperature activation energy, 0.95 ev, is roughly one half of the optical band gap of As_4Se_4 (viz. 2.0 $\pm$ 0.1 ev) and thus indicating the intrinsic conduction. To explain the conduction mechanism a possible alternative is also given considering two types of impurity states.

However the bulk glassy As_4Se_4 showed a single activation energy (0.98 ev) throughout the temperature range studied. This was attributed to the so called intrinsic behaviour resulting from the pinning of the Fermi level near the center of the gap as proposed for the amorphous semiconductors having gap states.

Generally, the impurities in amorphous semiconductors do not have noticeable effect on electrical conduction because the impurity atoms can accommodate themselves in the host matrix so that all the outer electrons will be taken up

in bonds. 2% of Cd, Zn, Ge and Sn in As_4Se_4 bulk showed no effect on electrical conduction. In all the cases only one activation energy ($\sim$ 0.97 ev) was observed which was quite comparable to the parent glassy As_4Se_4.

However 2% Ag in As_4Se_4 bulk gave two activation energies 0.20 and 0.55 ev whereas 2% of Cu in As_4Se_4 bulk gave the values 0.13 and 0.58 ev. In both the cases the reduction in activation energy was observed.

The optical absorption studies revealed that As_4Se_4 is a direct band gap material with the optical band gap 2.0 $\pm$ 0.1 ev.

In case of crystalline Sb_2Te_3 films the conductivity curve showed a single activation energy but as low as 0.12 ev whereas the optical band gap was reported to be 0.30 ev. We did not observe annealing effect as reported by earlier authors and thus ruled out the presence of grain boundaries in our samples. The Seebeck coefficient for Sb_2Te_3 was found to be 50 $\pm$ 20 μ V/^{o}K and was independent of temperature. The value of Seebeck coefficient suggested that the Fermi level was close to the valence band edge and the difference between them was $\sim$ 0.015 ev. The higher activation energy obtained from the conductivity measurements was attributed to be associated with mobility. The optical band gap was

found to be 0.27 ev for our films of crystalline Sb_2Te_3.

Antimony Selenide was amorphous and the conductivity curve showed a single activation energy equal to 0.42 ev whereas the optical band gap was found to be 1.25 ev. We could not reach the intrinsic range of conductivity for Sb_2Se_3. The small value of activation energy may be associated with some impurity level at 0.42 ev above the valence band as the material is p-type. The weak absorption below the edge suggest the absence of gap states. The activation energy may also be due to change in mobility with temperature as in a hopper. This point could be best resolved by measuring thermoemf or Hall effect as a function of temperature. Unfortunately we could not perform thermoemf measurements because of the high resistance of the sample.

The dependence of absorption coefficient on photon energy revealed that the amorphous Sb_2Se_3 has an indirect band gap of 1.25 ev.

Cadmium telluride was obtained in cubic form. The temperature dependence of conductivity showed a single activation energy 0.65 ev which was less than a half of the optical band gap (1.6 ev). We concluded that this activation energy 0.65 ev might be associated with impurity

level or crystal defect level.

The cubic CdSe films also gave a single activation energy 0.24 ev which was attributed to native imperfections in the crystalline films. The native imperfections might be arising from Se vacancies. The optical band gap for CdSe was found to be 1.75 ev.

Invariably, the optical absorption coefficient α, for all the compounds studied except amorphous Sb_2Se_3 obeyed the relation,

$$\alpha = \frac{C\,(h\nu - Eg\ opt)^{\frac{1}{2}}}{h\nu}$$

indicating the compounds were direct band gap. The amorphous Sb_2Se_3 showed the following dependence:

$$\alpha = \frac{C\,(h\nu - Eg\ opt)^{2}}{h\nu}$$

The amorphous Sb_2Se_3 gave an indirect band gap equal to 1.25 ev.

The chemical method of preparation of thin films of chalcogenides has its own merits which are summarised below.

(1) Large area uniform films can be obtained without any special provision.

(2) The films obtained were free from grain boundaries and voids which was examined under projection microscope.

(3) It has been observed in many cases that the thickness of the film increases with time (during the deposition) upto certain thickness beyond which no growth takes place. This upper limit of thickness retains for particular compound under particular experimental conditions. The advantage of this finding is to produce films of reproducible thickness for optical and electrical measurements.

(4) Above all, this method is so simple and easy that one can employ it to mass scale production of thin films. The same solution can be repeatedly used and thus the losses during the process are negligible and consequently the ultimate cost of production will be reduced considerably.

The above observations hopefully demonstrate the importance and usefulness of this chemical method of preparing thin films of semiconducting chalcogenides.

—oo 0 oo—

A C K N O W L E D G E M E N T

I am highly grateful to Dr. A. P. B. Sinha for his invaluable guidance during the course of this work.

Co-operation from my colleagues in many phases of this investigation is warmly acknowledged.

My thanks are also due to the Director, National Chemical Laboratory, Poona-8, for allowing me to submit this work in the form of thesis.

R.R.Khandekar
(R. R. KHANDEKAR)